University of Illinois at Urbana-Champaign

ACRC

Air Conditioning and Refrigeration Center A National Science Foundation/University Cooperative Research Center

Experimental Investigation of the Source of Acoustic Bursts Produced by Household Refrigerators

S. M. McLevige and N. R. Miller

ACRC TR-184 July 2001

For additional information:

Air Conditioning and Refrigeration Center
University of Illinois
Mechanical & Industrial Engineering Dept.
1206 West Green Street
Urbana, IL 61801

(217) 333-3115

Prepared as part of ACRC Project #105
Sound Generation Mechanisms in Expansion Devices
N. R. Miller, Principal Investigator

The Air Conditioning and Refrigeration Center was founded in 1988 with a grant from the estate of Richard W. Kritzer, the founder of Peerless of America Inc. A State of Illinois Technology Challenge Grant helped build the laboratory facilities. The ACRC receives continuing support from the Richard W. Kritzer Endowment and the National Science Foundation. The following organizations have also become sponsors of the Center.

Amana Refrigeration, Inc.
Arçelik A. S.
Brazeway, Inc.
Carrier Corporation
Copeland Corporation
Dacor
Daikin Industries, Ltd.
DaimlerChrysler Corporation
Delphi Harrison Thermal Systems
Frigidaire Company
General Electric Company
General Motors Corporation
Hill PHOENIX
Honeywell, Inc.
Hussmann Corporation
Hydro Aluminum Adrian, Inc.
Indiana Tube Corporation
Invensys Climate Controls
Kelon Electrical Holdings Co., Ltd.
Lennox International, Inc.
LG Electronics, Inc.
Modine Manufacturing Co.
Parker Hannifin Corporation
Peerless of America, Inc.
Samsung Electronics Co., Ltd.
Tecumseh Products Company
The Trane Company
Thermo King Corporation
Valeo, Inc.
Visteon Automotive Systems
Wolverine Tube, Inc.
York International, Inc.

For additional information:

Air Conditioning & Refrigeration Center
Mechanical & Industrial Engineering Dept.
University of Illinois
1206 West Green Street
Urbana, IL 61801

217 333 3115

Table of Contents

List of Figures

List of Tables

Chapter 1

1.0 Introduction

For many years, manufacturers of household refrigerators have been investigating a “popping” noise that occurs shortly after the compressor begins an on cycle. The noise has caused many service calls that would otherwise be unnecessary. Previous investigation of the “popping” has left many questions unanswered regarding possible causes of the noise and ways to avert it. Knowledge of the “popping” cause has been so illusive, recent work by manufactures has explored ways to muffle the noise rather then stop it.

The objective of this project is to experimentally investigate the phenomenon. A series of experimental investigations into the “popping” noise are described. They attempt to find the conditions surrounding “popping” and then to discern which conditions are important to the problem. The experimental investigation began with a refrigerator that regularly demonstrates the “popping” and was followed by experimental apparatuses that allowed control of various conditions while maintaining important features of the original system.

After investigating this problem in depth, the probable cause presented in this paper is condensation induced shock (CIS). The phenomenon of CIS in refrigeration systems has not been explored widely (3). Condensation shock is the cause of many similar problems in a variety of fields, including the nuclear power and chemical industries.

This paper explores the findings of these experimental investigations and the possibility of the “popping” noise being generated by CIS. Chapter 2 is dedicated to providing the reader an overview of important topics for CIS in refrigerators. Including transient refrigerant migration during the on and off cycle, vortex formation at hydraulic inlets, and CIS itself. Chapter 3 details the refrigerator experiments and their major findings. Chapter 4 and 5 describe the experimental apparatuses that were used to simulate the conditions under which “popping” occurs in refrigeration systems. Chapter 6 presents overall conclusions of these findings.

Chapter 2

2.0 Background Information

To study the possibility of condensation induced shock in the capillary tube of household refrigerators, a review of condensation induced shock and the conditions leading to its cause is important. Also, during the course of our experimental investigation, refrigerant migration in the household refrigerator and vortex formation at the capillary tube inlet have been identified as key elements of the "popping" problem. This chapter is a review of condensation induced shock, refrigerant migration in household refrigerators, and vortex formation at hydraulic intakes.

2.1 Condensation Induced Shock

Condensation induced shock (CIS) occurs when a vapor bubble is suddenly surrounded by sub-cooled liquid. If the vapor bubble collapses quickly enough to cause the liquid to crash together forming a shock wave, CIS has occurred. Figure 2.1 shows a simple illustration of CIS as it would possibly occur in the capillary tube of a household refrigerator. As long as liquid is present, the shock waves will then travel in both directions and possibly excite structures upstream and downstream. If the shock wave encounters another pocket of vapor, the shock wave will dissipate.

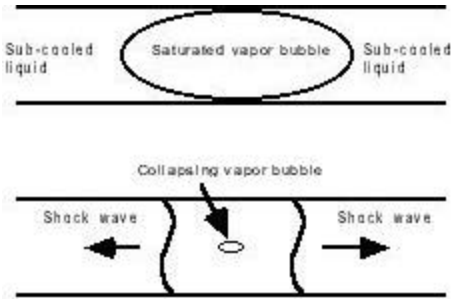

Fig. 2.1 - Condensation Induced Shock

The topics of bubble collapse and the excitation of a structure by the resulting shock wave have been studied theoretically and experimentally by a number of authors. Interest in bubble collapse has been largely due to the study of under water explosions and cavitation in pumps. Also, the excitation of a structure due to the resulting shock wave from CIS has been studied because in many applications CIS could not be designed out of the system. Therefore the systems needed to be designed to withstand the excitation.

Early study of CIS started in steam systems used in the power industry, chemical industry, and steam distribution where CIS is better known as two phase water hammer. Three types of conditions found to cause two-phase water hammer in steam systems have been noted by Kim 1987. They include line voiding, water columns separated by a vapor gap, such as at an elevated position, and slug flow induced trapping. Water hammer is a broader term that includes other shock mechanisms besides CIS like sudden valve closure. A wide variety of problems in a wide variety of fields have been attributed to water hammer. The discussion here will focus on bubble collapse and structure excitation caused by two-phase water hammer or CIS.

2.1.1 Bubble Collapse

The physical mechanisms of bubble collapse have been studied by a number of authors. Heat transfer and inertia both play an important role in the rate of collapse and the rate of collapse is directly related to the strength of the resulting shock wave. The inertial limit of the liquid is physically the fastest possible collapse while insufficient heat transfer will slow the collapse rate down. Much work has been done on determining whether conditions allow for an inertial controlled collapse or a heat transfer controlled collapse.

When heat transfer is good enough to absorb the heat from the collapsing bubble, the bubble collapse rate approaches its inertial limit. Rayleigh (1917) investigated the collapse of a spherical cavity in an incompressible fluid neglecting compressibility, viscosity, and surface tension. With no vapor to resist the collapse and the cavity being able to react instantaneously to pressure changes, Rayleigh's calculations provide an upper bound collapse rate. By solving equations of continuity and energy, Rayleigh came up with an equation of motion for the cavity wall:

$$U^2 = \frac{2P_L}{3r_L}\left(\frac{R_o^3}{R^3} - 1\right)$$

where: U = velocity of boundary
P_L = pressure of liquid
ρ_L = density of liquid
R_o = initial radius of boundary
R = time dependent radius of boundary

From this equation, the complete collapse time of any bubble that satisfies the given assumptions can be found by:

$$t = 0.91468R_o\sqrt{\frac{r_L}{P_L}}$$

He then goes on to solve for the resulting pressure field surrounding the collapsing cavity. At the initial stages of the collapse, the maximum pressure is found at infinity but as the collapse continues the maximum pressure is given by:

$$\frac{P}{P_{Lo}} = \frac{R_o^3}{\frac{4}{3}R^3}$$

where: P = time dependent pressure
P_{Lo} = initial pressure of liquid

which is now located at a finite radius given by:

$$r = 1.587R$$

Rayleigh's model does not account for compressibility and therefore as the collapse reaches completion the pressures goes to infinity. Rayleigh's model for an inertially controlled empty cavity collapse served as a starting point for further models.

Zwick and Plesset (1955) investigated the effect of heat transfer on bubble collapse. They numerically solved the equations of motion for the bubble wall and found that heat transfer did not play an important role in the conditions being investigated. It was later noted by Florshuetz and Chao (1965) that Zwick and Plesset's solution was correct for the bubble collapse conditions presented for their particular case, but heat transfer is not negligible in all cases. Zwick and Plesset (1955) also note that the assumption of dynamic and thermal equilibrium breaks down near the sonic velocity of the vapor. That is, initially the bubble collapses proceeds at a slow enough pace that all gas inside the bubble is able to condense allowing the internal vapor pressure to remain constant. At later stages of collapse if the collapse rate approaches the sonic velocity of the vapor, the gas does not have time to condense and the vapor pressure inside the bubble rises. This rise of internal pressure impedes the collapse and the internal vapor pressure grows to a value larger then the surrounding liquid causing the bubble to rebound.

Hunter (1960) considered compressibility affects in the collapse of the empty cavity neglecting surface tension and viscosity. Hunter found that in the compressible case the velocity of collapse must be of lesser order then the incompressible case. Also, the compressible solution allows for a shock wave to form and travel outwards from the collapse point.

Hickling and Plesset (1964) take into account compressibility and the presence of a small amount of gas inside the bubble. They found that as the amount of gas inside the bubble increases the velocity of the bubble wall near the end of collapse decreases, which reduces the strength of the collapse. Also, reducing the surrounding liquid pressure has the same affect of reducing the bubble wall velocity near the end of the collapse. Of larger importance was whether the gas was isothermal (able to remove the heat of compression) or the gas retained some of the heat of compression during the collapse. Isothermal bubble collapse had much higher bubble wall speeds at the end of collapse. Their model also predicted the creation of a shock wave. In their model, the liquid rebounds at the end of collapse and a compression wave forms a shock wave which propagates into the liquid.

The strength of the resulting shock is dependent on a number of properties, which include fluid properties and speed of bubble collapse. For a given set of fluid properties, the speed of collapse is related to the heat transfer with the collapse rate increasing with increasing heat transfer. When heat transfer is large enough, the upper limit of collapse rate is reached and the bubble collapses near the fluid's inertial limit. Before the inertial limit is reached, the speed of bubble collapse is related to the heat transfer between the vapor bubble and the surrounding liquid. A useful relation to determine how much heat transfer is present is the Jakob number, which is defined as (Jacobi and Shelton, 1995):

$$Ja = \frac{r_L c_L \left(T_S - T_L\right)}{r_G h_{fg}}$$

where: ρ_L = density of liquid
ρ_G = density of gas
h_{fg} = latent heat
c_L = specific heat of liquid
T_s = saturation temperature
T_L = temperature of liquid

This simply relates the amount of heat transfer from the bubble into the liquid to the amount of heat transfer needed for the vapor to condense to liquid. A higher Jakob number means that the possible heat transfer into the liquid is much higher then the heat transfer needed to condense the vapor. Thus, a higher Jakob's number means a faster condensation rate (Jacobi and Shelton, 1995).

Florschuetz and Chao (1965) explored the relative importance of heat transfer and inertia to the rate of bubble collapse. They came up with a dimensionless constant that can be used to determine whether the bubble collapse is more dependent on heat transfer or inertia. The constant is given by:

$$B_{eff} = y^{2}[Ja]^{2}\frac{k}{R_o}\left(\frac{r}{\Delta p}\right)^{1/2}$$

where: ψ = temperature difference correction factor
Ja = Jacobs number
κ = thermal diffusivity of liquid
ρ = density of liquid
Δp = difference between bubble saturation pressure and external pressure

As B_{eff} decreases, heat transfer effects become more important and as B_{eff} increases inertial effects of the liquid begin to dominate the collapse rate. They propose a classification of $B_{eff}<0.05$ as heat transfer controlled and $B_{eff}>10$ for inertia controlled. Values that fall between exhibit characteristics of both heat transfer controlled and inertial controlled collapse. The proposed classification is summarized in figure 2.2.

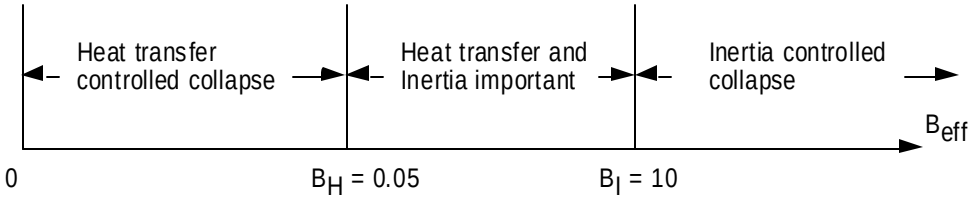

Figure 2.2 - Proposed classification by Florschuetz and Chao (1965)

Wittke and Chao (1967) studied the effect of translatory motion on bubble collapse. They studied the effect analytically and then experimentally. They found that bubble collapse is enhanced by translatory motion due to the increase in heat transfer. Situations with small Jakobs number are enhanced to a greater extent because the heat transfer due to the translatory motion accounts for a larger percentage of the total heat transfer.

2.1.2 Excitation of Structure

When prevention of CIS is not possible, engineers are concerned with the effect of the resulting shock wave on a particular piping system. Analysis of the effect of CIS in piping systems involves solving the fluid dynamics of the event coupled with the dynamics of the structure to obtain the time dependent response. The coupled equations are complex and take great computational effort even for a computer. Because of the complexities of the coupled equations, usually the response of the fluid and structure are decoupled and solved separately. (Gillessen, R et al, 1988) Solving the fluid dynamics involves solutions to mass conservation, pulse conservation, and energy conservation. These partial differential equations are usually solved with the aid of a

computer. The response of the structure is then found using a finite element model. Hatfield and Wiggert (1982), Sibetheros et al (1991), Walker and Phillips (1977), Belytschko et al (1986), and Suo and Wylie (1989), are among people who have investigated calculating the response of a piping system to transient pressure fluctuations found in CIS.

The most common way to solve for the unsteady flow associated with the fluid transients found in CIS is the characteristic method. The continuity and momentum equations for the liquid yield partial differential equations with velocity and hydraulic grade line as dependent variables. The characteristic method transforms these into four ordinary differential equations. (Wylie et al, 1978) The unsteady flow solutions, which are usually numerically solved, give pressure forces on the piping, which can then be used to solve a structural analysis. Sibetheroset et al (1991) investigated the use of spline polynomials in the numerical solution to the method of characteristics.

The method described above of applying the solution of the method of characteristics to a structural analysis assumes that the fluid is incompressible. The assumption of incompressibility of the fluid is thought to assure the solution yields an upper bound stress level because fluid-structure interactions should reduce the true level of stress. Belytchko et al (1986) investigated the assumption of incompressibility of the fluid. They found that the assumption held for simple piping systems, but for complex systems the incompressibility assumption could sometimes result in lower prediction of loads and stresses. They present a way to include acoustic properties of the fluid into the predicted response of flexible piping. A similar investigation into the effects of frequency dependent variables and how to incorporate the effects into a model was done by Suo et al (1989).

Hatfield and Wiggert (1991) use a technique they call component synthesis, which solves the structural analysis before the hydrodynamic analysis. The technique involves creating a standard finite element model and solving for the modes, mode shapes, and stiffness of the overall system. The system is broken up into the overall system and liquid components. The overall system includes the pipes, supporting structure, and mass of liquid transverse to the pipes. Liquid components represent the liquid between junctions. The modal parameters found by solving the structural finite element modal are then used as an input to the hydrodynamic analysis, which involves the method of characteristics.

Gillessen et al (1988) discusses possible piping design to lessen the effect of the shock. The use of a more rigid material (high modulus of elasticity) can help keep the resonance frequency from being excited. The piping can also be designed to absorb the excitation.

The above discussion of possible ways to predict the response of a particular piping system is intended to inform those interested of different methods available. The above methods could be very useful to individual designers to determine how the system could be changed to reduce the “popping” noise.

2.1.3 Condensation Induced Shock in Refrigeration Systems

Not much work has been done in the area of CIS in refrigeration systems (Jacobi and Shelton, 1997). Some early work dealing with pressure spikes in refrigerant compressors may have been the result of CIS such as Singh, et al (1986). Jacobi and Shelton investigated CIS in ammonia systems and their results and literature search can be found in Jacobi and Shelton (1997) and Jacobi and Shelton (1995). In ammonia systems, hydraulic shocks

were found to occur at the beginning and end of the hot gas defrost cycle. The shocks were possibly caused by CIS when the hot gas entered the evaporator and came into contact with cold condensate.

2.2 Refrigerant Transients

The "popping" problem occurs at the beginning of the compressor-on cycle of the household refrigerator. At this time, the system has not reached steady state. The system is transitioning from the off cycle conditions to the steady state conditions. This means, the conditions just before the compressor turns on are the initial conditions to the transient period containing the "popping" event. This transient period is characterized by a redistribution of refrigerant to steady state conditions. The migration of refrigerant at start-up and shut-down has been investigated in the past for the purpose of calculating cycling losses in household refrigerators and their insights into refrigerant migration are useful here.

Household refrigeration cycle losses were investigated experimentally by Wang and Wu (1990), Rubas and Bullard (1995), and Coulter and Bullard (1997). They found that the system reaches a steady state pressure in the off cycle corresponding to the saturation temperature in the evaporator which means that vapor exists in any component with a temperature above the saturation temperature found in the evaporator. If sufficient time has passed, all components that are not in the freezer compartment have an off cycle equilibrium temperature equal to the atmospheric temperature and thus are filled with vapor. During the steady state run cycle, much of the refrigerant resides as liquid in the condenser. Because vapor can only exist in the condenser during the off cycle, the refrigerant must redistribute upon shut-down. In Rubas and Bullard (1995), refrigerant was found to migrate through the capillary tube after the compressor turned off. The migration began with liquid entering the capillary tube followed by vapor as the pressure difference across the capillary tube decreased. The migration continued as long as a pressure difference across the capillary tube existed. 95% of the refrigerant found in the condenser at the end of the compressor-on cycle was found to migrate into the evaporator.

The refrigerant that migrates during the compressor-off cycle must be redistributed at the beginning of the next compressor-on cycle before the system can reach steady state. Initially after the compressor turns on, two phase refrigerant leaves the evaporator (Rubas and Bullard, 1995). The quality of the two-phase refrigerant leaving the evaporator is unknown. In Rubas and Bullard (1995), a microphone was used to determine if liquid could be heard exiting the evaporator. They reported hearing possible slugs of liquid passing by the microphone, but they believe much of the refrigerant leaves in the form of high quality two-phase.

The popping problem occurs at the beginning of the compressor-on cycle and therefore is directly related to these refrigerant transients. The conditions just before the compressor turns on and how the refrigerant is redistributed will later provide insight into system temperature transients occurring during the compressor start-up. We will see later that the redistribution of refrigerant is one key factor of the popping event.

2.3 Vortex Flow

The experimental investigation of the "popping" noise has lead to the examination of vapor entraining vortices occurring at the capillary tube inlet as a possible source of bubbles for CIS. Gas entraining vortices at hydraulic intakes have been investigated for larger applications such as that found in the electric power industry. (Tsou et al, 1994). The vast majority of studies on gas entraining vortices deal with sump pumps, which have the

inlet inverted relative to the capillary tube application. In pumps, air entrainment causes pump wear and in severe cases pump failure.

Gas entraining vortex flow can occur when the flow transitions from a free surface to pressure flow conditions near a hydraulic intake (such as the capillary tube inlet) (Knauss,1987). The surface vortices are reported to have a number of causes including eccentric orientation of the intake, non-uniform approach of flow toward the intake, flow obstructions, and unsteady flow (Knauss,1987). Tsou et al (1994) begins by defining terms commonly encountered concerning vortices at hydraulic intakes such as swirl, circulation, and vorticity. Swirl is a basic term used to describe the rotation of a particular flow. Circulation is a formal flow property, which describes the net vorticity over a region. Vorticity is also a formal flow property, which describes the magnitude of angular velocity about a certain axis in a region of flow.

Early experimental work with air entraining vortices in sump pumps was carried out by Denny (1956). Figure 2.3 represents a simple diagram of his experimental set up. The setup is different from the capillary inlet (the inlet is inverted to the free surface), but his results are noteworthy.

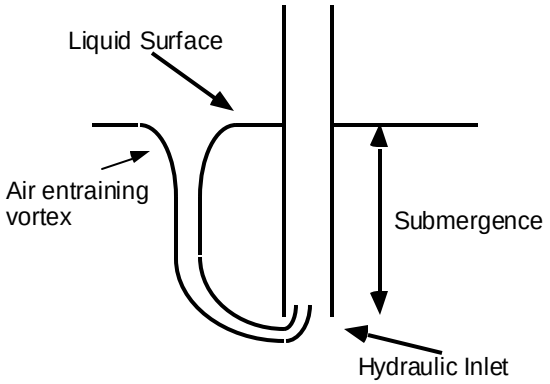

Figure 2.3 - Diagram of sump pump vortices studied by Denny (1956)

His experiments compared the pump aspects of inlet flow velocity, inlet swirl, and inlet shape to critical submergence depth of the hydraulic inlet to avoid an air-entraining vortex. Critical submergence is the minimum depth for which air-entraining vortices do not form with an increase in inlet flow velocity. Figure 2.4 is a typical plot of his vortex data and shows how as inlet velocity increases the submergence depth needed to avoid an air entraining vortex grows. Eventually, a critical submergence depth is reached where no air is entrained no matter how much the inlet velocity is increased. Similar plots were made to compare the other aspects of the pump. For his particular experiment, he found that reducing the swirl of incoming liquid to the pump inlet reduced the critical submergence by a factor of four. The experiment with inlet shape found that a straight walled inlet had a shallower critical submergence, but formed air-entraining vortices more readily at slower inlet velocities.

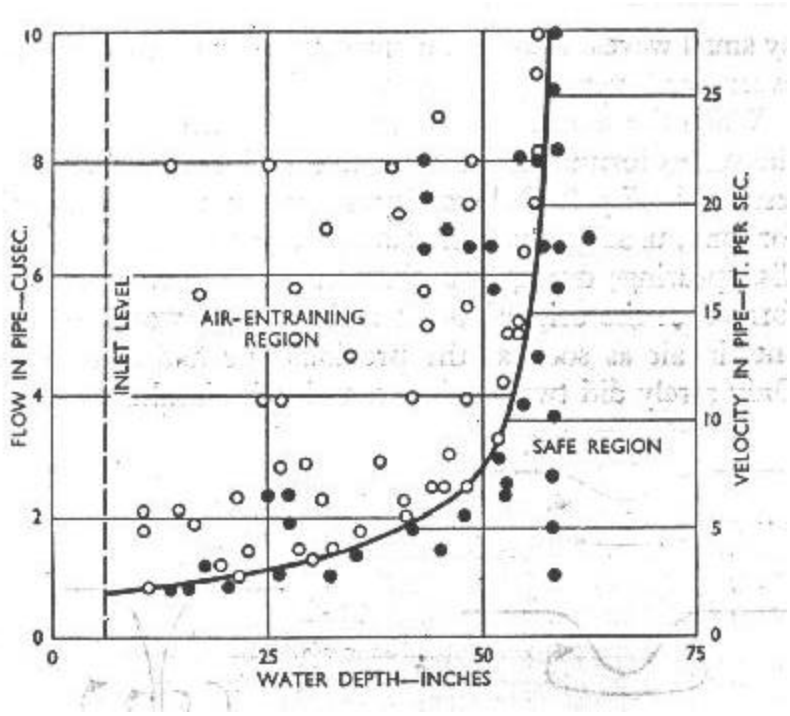

Figure 2.4 - Plot of inlet velocity vs. submergence to show whether air entraining vortices were present (Denny, 1956)

The Hydraulic Institute Standards (1983) reviewed methods of stopping air-entraining vortices in sump pumps. It offers some general guide lines to reducing inlet vortices:

i) Reduce inlet flow velocity to the hydraulic inlet holding vessel

ii) Reduce flow velocity into the hydraulic inlet

iii) Change geometry of inlet so that inlet flow to hydraulic vessel does not add swirl to the flow

Knauss (1987) discusses using vortex suppressors to eliminate air-entraining vortices in sump pumps. The basic function of the vortex suppressors is to prevent the flow from swirling at and around the sump inlet, which means the suppressors could be possibly adapted to the capillary tube geometry. Horizontal grating, floating rafts, and caging are given as effective examples of vortex suppressors.

Durgin and Hecker (1978) looked at scaling of experimental models of hydraulic intakes experiencing vortex flow. They provide a review of swirl origination and sight three main sources:

I) Offset of incoming flow from the inlet

II) Velocity gradients at the inlet - "viscous induced velocity profiles are inherently rotational with the wall itself a vorticity source."

III) Obstruction around the inlet

The capillary tube inlet is not offset from the incoming flow and there are no obstructions in the very near vicinity of the inlet. Velocity gradients at the inlet of the capillary tube could be a possible source of the inlet vortex. Although no attempt to measure the velocity distribution about the inlet, simple observations show that liquid in the near vicinity of the inlet moves rapidly toward the inlet. Liquid near the filter dryer wall seems to be stagnate, but no attempt to verify this observation was made.

Gas entrainment at the free surface of a liquid was studied by Takahashi et al (1988). Their experiment consisted of a cylindrical vessel with vertical intake projecting into the vessel, which is geometrically similar to the capillary inlet case. They witnessed three different mechanisms:

(A) "Vortex-induced entrainment"

(B) "Conically depressed surface with entrainment of relatively large round bubbles"

(C) "Falling flow along pipe accompanied by entrainment of fine bubbles"

Type A occurs at low inlet velocities and relatively large submergence. Its physical appearance is characterized by a shallow vortex on the liquid surface and a thin core of gas reaching to the inlet. Type B occurs at high inlet velocities and for small diameter intakes. Its physical appearance is characterized by a conical dip in the free surface and relatively large bubbles detaching from the apex and entering the inlet. Type C occurs at low submergence, high inlet velocities, and large inlet diameter. A column of vapor reaching well into the inlet characterizes type C.

Type B holds possible significance to condensation induced shock. If present at the capillary tube inlet, this type could entrain relatively large bubbles into the capillary tube flow as in figure 2.5. Takahashi et al (1988) took a picture of this type of entrainment and it can be seen in figure 2.6.

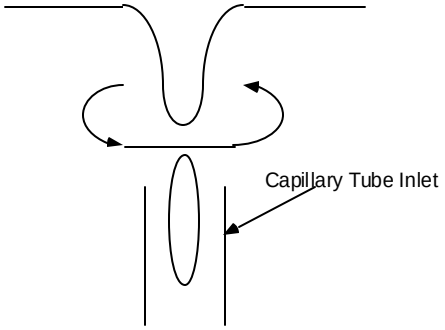

Figure 2.5 - Bubble entrainment

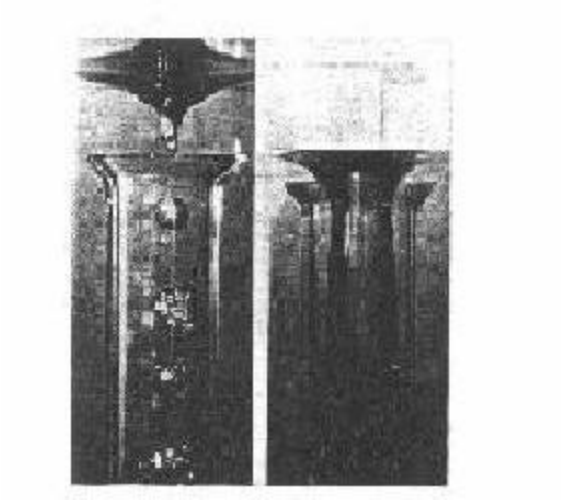

Figure 2.6 - Picture of vortex entraining bubbles (Takahashi et al, 1988)

Chapter 3

3.0 Refrigerator experimentation

An experimental investigation was conducted to determine the source of the "popping" noise reported by refrigerator manufacturers. In the past, the manufacturers had difficulty studying the popping problem due to the sensitivity of the problem. Small changes in the system would stop the "popping" and thus make the experiment void. A refrigerator that experiences the "popping" problem was obtained from an ACRC center member and an attempt was made to define the important elements of the problem. After obtaining the operating conditions of the refrigerator during the "popping" event, a hypothesis was made followed by more experimental investigation to try to prove or disprove the hypothesis.

3.1 Refrigerator Instrumentation

A refrigeration unit that continually experiences the popping noise was donated. An Amana household refrigerator model TR25V2W was instrumented to identify the operating conditions under which the capillary tube "popping" noise occurs. Figure 3.1 shows a schematic of the refrigerator with some important transducers shown.

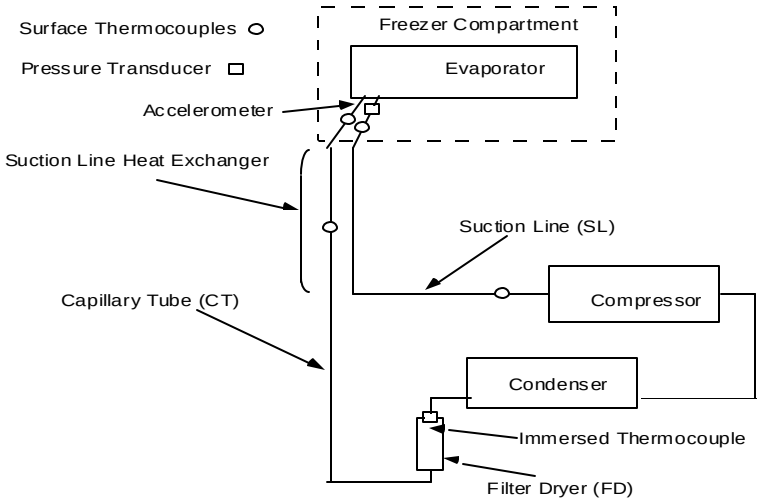

Fig. 3.1 - Refrigerator instrumentation

To study this phenomenon, the refrigerator was instrumented to capture the temperature and pressure conditions of the refrigerator components while being as non-invasive as possible so as to not affect the popping. Table 3.1 contains a list of surface thermocouples along with their locations (not all thermocouples in the table are represented in Fig. 3.1).

Table 3.1

Thermocouples	Location	Name in Plots
Capillary Tube Exit	Located on connection between capillary tube and evaporator	CT Exit
Capillary Tube Inlet	Located 8 inches downstream of the evaporator on the capillary tube	CT Inlet 8" after FD
Suction Line Inlet	Located on the connection between the evaporator and suction line	SL Inlet
Suction Line Exit	Located 12 inches upstream of the compressor	SL Exit 12" to Comp
Suction Line Heat Exchanger Middle	Located on the capillary tube as it enters the suction line heat exchanger	Not shown in plots
Suction Line Heat Exchanger Near Evaporator	Located on the capillary tube as it leaves the suction line heat exchanger	Not shown in plots
Condenser Middle	Located on the condenser tube approximately 1/3 of condenser length away from the exit	Not shown in plots

An immersed thermocouple was installed in the filter dryer to provide better temperature reading at the inlet to the capillary tube and is labeled FD Top in the plots. The pressure transducers are located on the suction line inlet and a filter dryer filling port. Figure 3.2 shows the instrumentation on the filter dryer, which gives the conditions at the inlet to the capillary tube. With these locations, the exact pressure in the filter dryer and at the inlet to the suction line is known. Using these pressures, approximate pressures are known at the inlet to the capillary tube and throughout the evaporator.

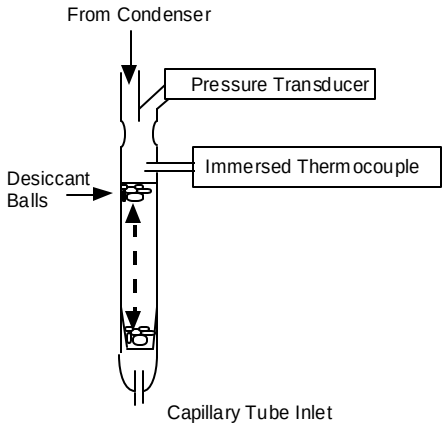

Fig. 3.2 - Instrumentation on the filter dryer

3.2 Capturing the Pop

To measure when a "popping" event occurs, an accelerometer was placed on the sleeve that connected the capillary tube to the evaporator. Fig. 3.3 shows a simple diagram of how the accelerometer was mounted. The mounting washer was adhered to the sleeve with adhesive. This position was chosen because relatively large surface acceleration could be captured here. The pop was also captured at many other accelerometer positions, but

the capturing of the pop was used for timing purpose rather then to study the dynamics of the event. Therefore the simple detection of the pop was sufficient for this study.

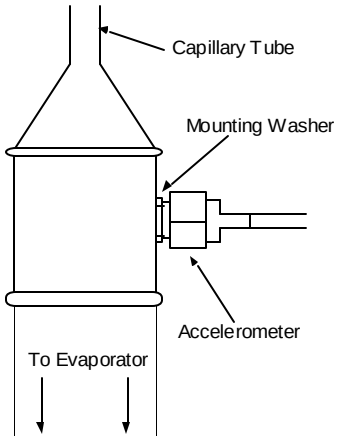

Figure 3.3 - Mounting of accelerometer

3.3 Experimental Data

Figure 3.4 shows a temperature profile for the entire compressor-on cycle. The x-axis shows time in seconds with t=0 is the time the compressor turns on. The approximate time the pop occurs is labeled and the figure shows that the refrigerator is experiencing large temperature gradients throughout the system at the time of the pop. The pressure in the filter dryer is shown on the plot converted to saturation temperature.

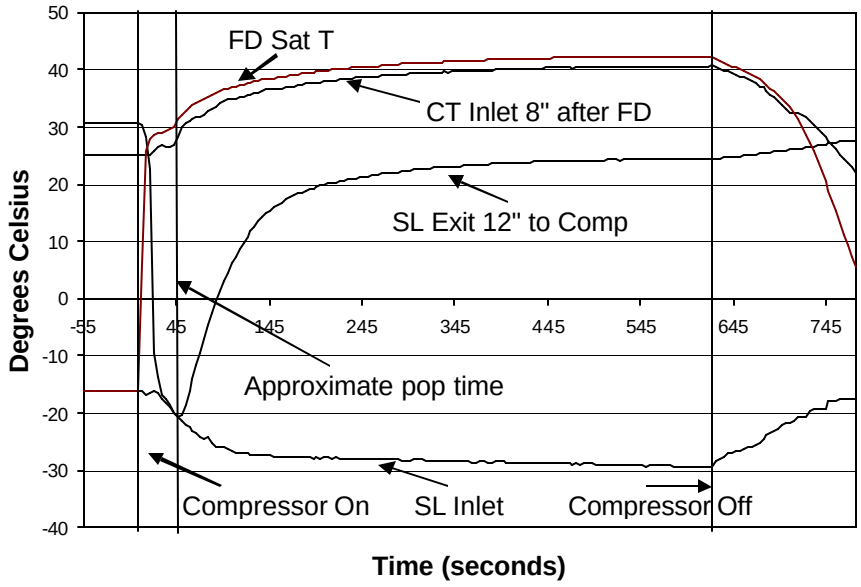

Figure 3.4 - Temperature plot of compressor on cycle

Figure 3.5 shows the pressure profiles as measured by the pressure transducers on the filter dryer and the entrance to the suction line. Notice that the pressure of the filter dryer is approximately 110 psi at the time of the

pop which means the high side pressure has only reached a level of about 75% of it's final value. The pressure at the inlet to the suction line is still dropping at the popping point as well.

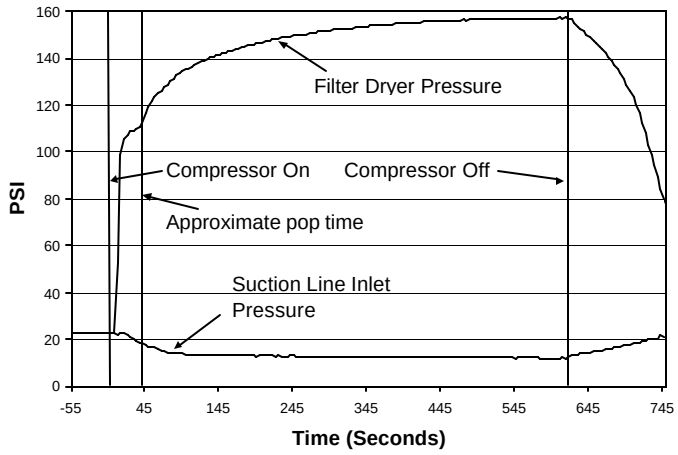

Figure 3.5 - Pressure plot of compressor on cycle

Notice in figure 3.4 that the suction line exit surface temperature drops down to near the suction line inlet temperature very quickly after the compressor-run cycle begins. The suction line exit surface thermocouple is located approximately 12 in from the end of the suction line which means that the suction line has dropped to or below that temperature along the entire length of the suction line heat exchanger. The surface temperature of the suction line heat exchanger does not begin to warm up until about 50 seconds after the compressor has turned on and after the popping event has ended. Thermocouples placed along the suction line heat exchanger on the capillary tube also have shown this drop in temperature.

As previously discussed in section 2.2, a redistribution of refrigerant is occurring at the start of the compressor-on cycle. Excess refrigerant that pooled in the evaporator during the compressor-off cycle is now being redistributed at the start of the compressor-on cycle. This refrigerant leaves at the saturation temperature in the evaporator and thus cools the suction line heat exchanger dramatically. Also as discussed earlier, the condenser begins the compressor-on cycle filled with vapor and thus for a time only vapor enters the capillary tube at the start of the compressor on cycle. With the cross sectional area of the suction line approximately 48 times as large as the cross sectional area of the capillary tube and when only vapor is entering the capillary tube, the suction line dominates the suction line heat exchanger temperature at the start of the compressor-on cycle. Refrigerant then begins to build in the condenser due to the increasing pressure and refrigerant redistribution. Eventually, liquid begins to enter the capillary tube and the quality of refrigerant leaving the evaporator has increased so that the suction line heat exchanger temperature begins to rise to its steady state value.

Figure 3.6 highlights the temperature and pressure profiles of the first 65 seconds of the start cycle. The approximate pop time for this specific cycle is marked on the plot. At the time of the "popping" the suction line heat exchanger temperature was suppressed to the evaporator temperature. This momentary temperature drop of the suction line is believed to be one key parameter of the "popping" noise.

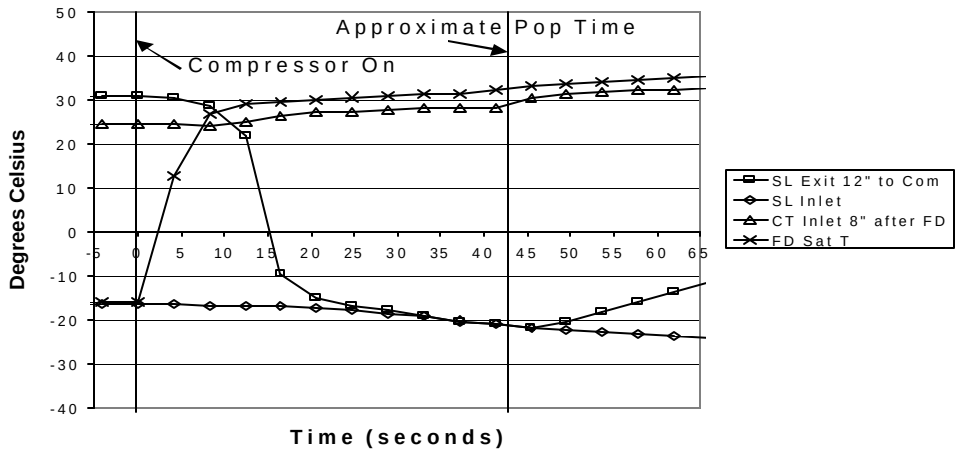

Figure 3.6 - Temperature plot of entire compressor on cycle

A plot of the "popping" as captured by an accelerometer located on the surface of the capillary tube near its exit is shown in figure 3.7. The "popping" noise can simultaneously be heard audibly while this surface acceleration of the capillary tube exit is recorded. It is believed this acceleration vs. time plot represents the impulse response of the refrigeration components as measured by the surface accelerometer.

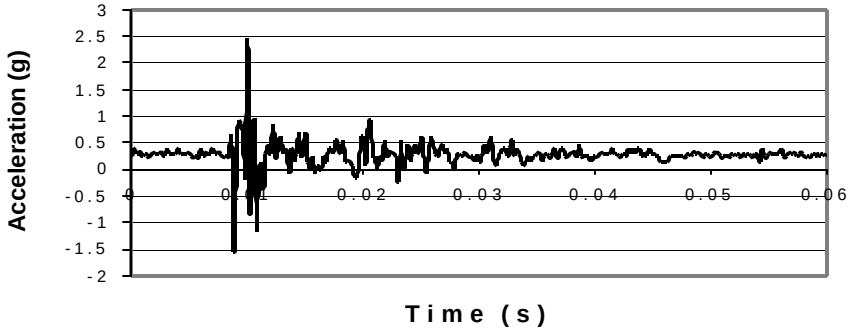

Figure 3.7 - Acceleration vs. Time at the capillary tube exit

3.4 Popping Noise Hypothesis

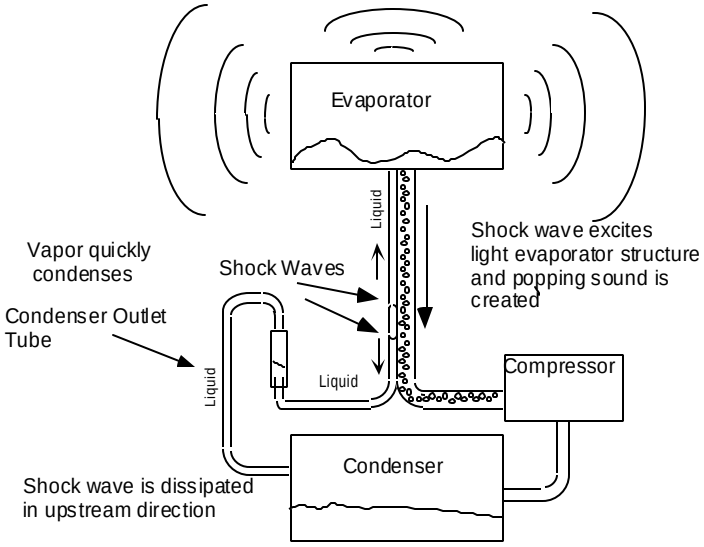

Fig. 3.8 - Depiction of popping event

The presence of vapor in the capillary tube, the drop in temperature of the suction line heat exchanger, and the large system transients at the time of the "popping" lead to the hypothesis of condensation induced shock causing the "popping" event. Fig. 3.8 shows how condensation induced shock could occur during the compressor start-up cycle of the refrigerator. As discussed in section 2.2, refrigerant pools in the evaporator during the off cycle and only vapor is present in all components not at or below the evaporator temperature. This means that only vapor exists in all components outside the freezer compartment. At start-up of the compressor, a redistribution of refrigerant takes place causing large pressure and temperature transients in the system.

At start-up, the evaporator empties the excess refrigerant through the suction line. At this same time, the pressure in the condenser is rising and refrigerant begins to pool in the condenser. Until the condenser is able to output a sufficient amount of liquid, only vapor enters the capillary tube. This causes the suction line heat exchanger to drop to a nearly the evaporator temperature. The temperature along the suction line heat exchanger remains at nearly the evaporator temperature until the refrigerant redistributes and liquid begins entering the capillary tube while vapor begins to enter the suction line.

Some time approximately 30-50 seconds after the beginning of the compressor-on cycle when the vapor flow is transitioning to liquid flow at the capillary tube inlet, vapor bubbles enter the capillary tube and travel to the suction line heat exchanger. Here it is not certain exactly what happens. One possibility is that as the bubbles enter the suction line heat exchanger very good heat transfer exists between the capillary tube wall and the liquid surrounding the bubbles and therefore the liquid temperature drops very quickly. The vapor bubbles then find themselves surrounded by relatively cold sub-cooled liquid. This leads to the conditions associated with condensation induced shock. The vapor bubble quickly collapses causing shock waves to propagate in both the up and down stream direction.

The magnitude of the shock would vary according to the properties of condensation induced shock. As discussed in section 2.1, properties like bubble size, speed of collapse, and temperature gradient between the vapor and liquid phase play an important role. The shock wave would travel upstream and downstream. The shock wave is able to excite components in the downstream section causing the "popping" noise to be heard audibly. The upstream shock wave is never heard audibly, and is probably dissipated. Possible explanations include impacting another vapor pocket or being unable to sufficiently excite the upstream components to produce an audible event.

3.5 Conditions at Inlet and Outlet of Capillary Tube

A closer look at the temperature and pressure data can give a better idea of what is happening at the inlet and outlet of the capillary tube. Temperature and saturation temperature in the filter dryer can be viewed in figure 3.9 and corresponds to the capillary inlet conditions. The figure shows that while the compressor is off, the filter dryer is filled with superheated vapor. After the compressor turns on, the pressure (and thus the saturation temperature) begins to rise and two-phase liquid enters the filter dryer. At this point, the pressure seems to level off for 20 to 30 seconds. Eventually, the condenser fills with liquid sufficiently such that only liquid enters the filter dryer and so the capillary inlet is sealed by liquid. As the liquid covers the capillary tube inlet, the pressure in the filter dryer begins to rise again and continues to rise until it reaches the compressor-on equilibrium pressure.

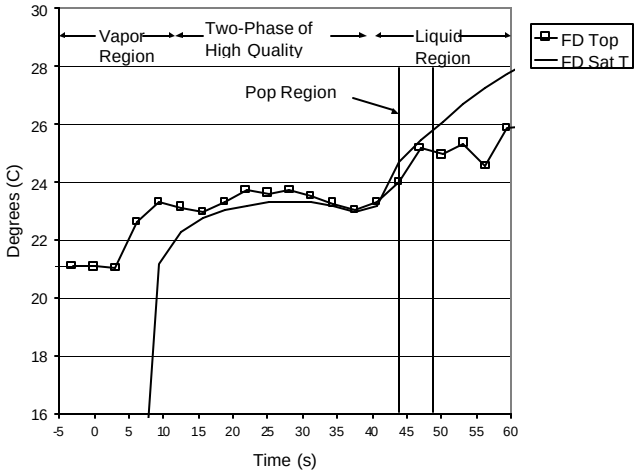

Figure 3.9 - Capillary tube inlet conditions

An ACRC member installed a glass filter dryer to visually see what was happening at the start of the compressor-on cycle. The filter dryer began filled with vapor as the data showed. In agreement with the data, the flow then transitioned to two-phase flow. The two phase was mainly saturated vapor with a small amount of liquid entering the filter dryer, but not enough to come near covering the inlet to the capillary tube. Then at a point corresponding to the start of the liquid region in the data, liquid filled the filter dryer and covered the capillary tube inlet. The mass flow of liquid entering the filter dryer was inconsistent allowing for covering, uncovering, and recovering of the capillary tube inlet. As the system moved towards steady state the mass flow became more consistent.

An interesting phenomenon was observed shortly after the capillary tube was first covered with liquid. Many times, complete uncovering of the capillary tube did not occur and as the liquid level neared the capillary tube inlet a vortex formed. This vortex seemed to be directly related to the popping noise. Upon appearance of the vortex, the "popping" noise could be heard. The appearance of the vortex is believed to be an important part of the "popping" problem and will be explored further in chapter 4.

Figure 3.10 represents the approximate temperature and pressure at the capillary tube exit. The temperature was measured by a well-insulated surface thermocouple placed at the exit region. The pressure was measured at the exit of the evaporator so that the actual pressure at the capillary tube exit is a little higher due to pressure drop across the evaporator. A region where liquid is believed to exit the capillary tube is labeled on the figure. Due to the limit in accuracy of the instrumentation, it can not be known conclusively form this data that liquid does exit the capillary tube during the labeled region. However, Figure 3.10 compares the surface temperature at the exit of the capillary tube and the saturation temperature at the exit of the evaporator. Thus the saturation temperature at the exit of the capillary tube probably resides somewhere above the saturation temperature on the figure due to some pressure drop across the evaporator. Liquid exiting the capillary tube would allow a shock wave to propagate into the evaporator.

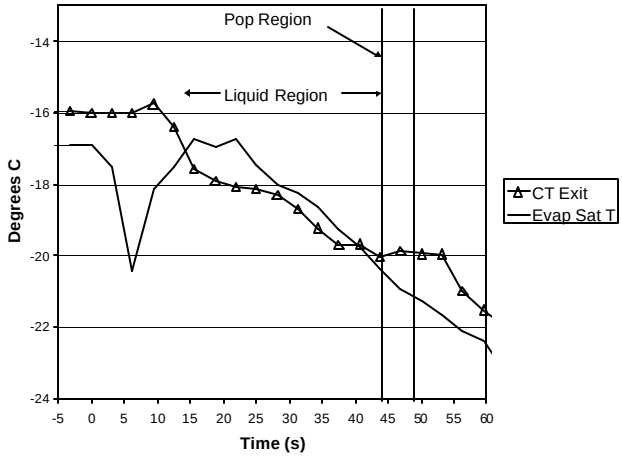

Figure 3.10 - Suction line inlet

3.6 Further Experimentation

From the previous data and observations, two important events were identified. The formation of a vortex at the capillary tube inlet and the drop in temperature of the suction line inlet seemed to correspond directly to the "popping" phenomena. Simple experiments were then conducted to test their relationship to the "popping" problem.

3.6.1 Horizontal and vertical filter dryer

Moving the filter dryer to a horizontal position, thus changing the capillary tube inlet to a horizontal position, caused the "popping" event to cease. Figure 3.11 contains photographs of the filter dryer in the vertical and horizontal position. The filter dryer is made of copper, but in the picture it is covered in black insulation. Experimentally moving the filter dryer from vertical, to horizontal, and back to vertical on consecutive cycles controlled the popping. The position of the filter dryer was changed during the off cycle. During the next run cycle,

the unit popped when the filter dryer was in the vertical position and did not pop when the filter dryer was moved to the horizontal position.

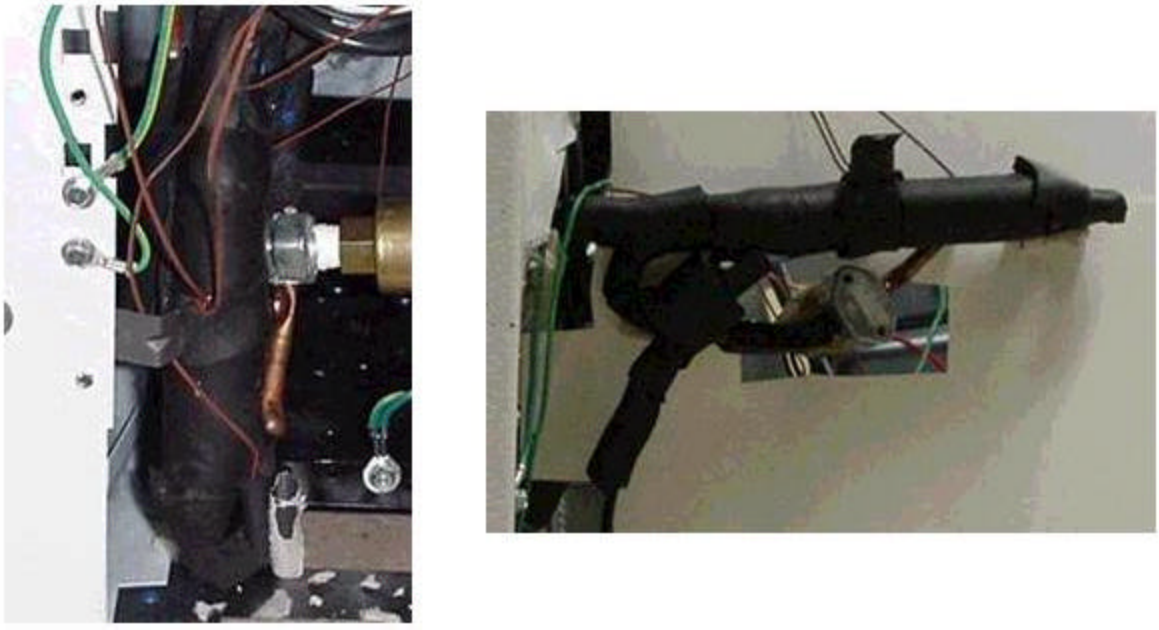

Figure 3.11 - Filter dryer in vertical position and in horizontal position

Figures 3.12a and 3.12b represent the temperature profiles of the system during the repositioning of the capillary tube inlet. The two plots are nearly indistinguishable from each other. Moving the filter dryer did not change any of the temperature or pressures being measured on the system. Yet, the popping would not occur when the filter dryer was moved to the horizontal position.

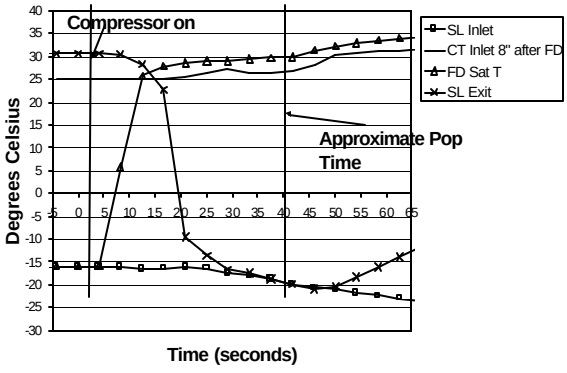

Figure 3.11a - Vertical Filter Dryer

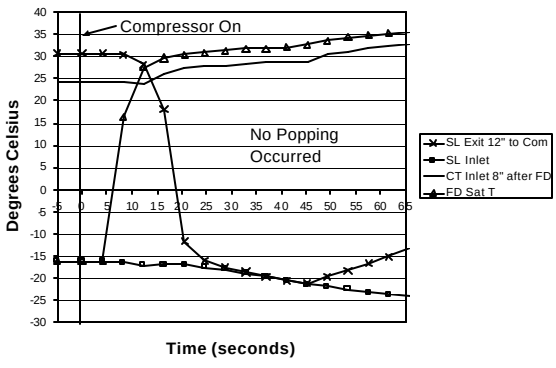

Figure 3.11b - Horizontal Filter Dryer

It remains a possibility that the instrumentation did not capture the pressure or temperature change in the system caused by moving the filter dryer to the horizontal position. However, it is believed that better explanation can be found by studying the vortex at the capillary tube inlet. In the clear filter dryer, one could see that a vortex

would form during the start cycle. With the filter dryer in the vertical position, a vortex forms and was able to entrain bubbles into the flow at the capillary tube inlet. The bubble then traveled down the capillary tube to the suction line heat exchanger where they collapsed in the form of condensation induced shock. Bubble entrainment by vortices has been studied extensively as is previously noted in section 2.3. Placing the filter dryer on its side, a vortex may not have been able to form and thus no bubbles were entrained.

3.6.2 Experimental Warming of Suction Line Heat Exchanger

To test the importance of the drop in temperature of the suction line heat exchanger, an experiment was designed to limit the drop in temperature. Experimentally, the "popping" could be suppressed by clamping a tube to the suction line heat exchanger so that room temperature coolant could be used to warm the suction line heat exchanger as in figure 3.12. If the warming tube was drained, the refrigerator continued to pop during a start cycle. It is believed that the warmed suction line heat exchanger no longer gave the conditions necessary to support popping due to condensation induced shock.

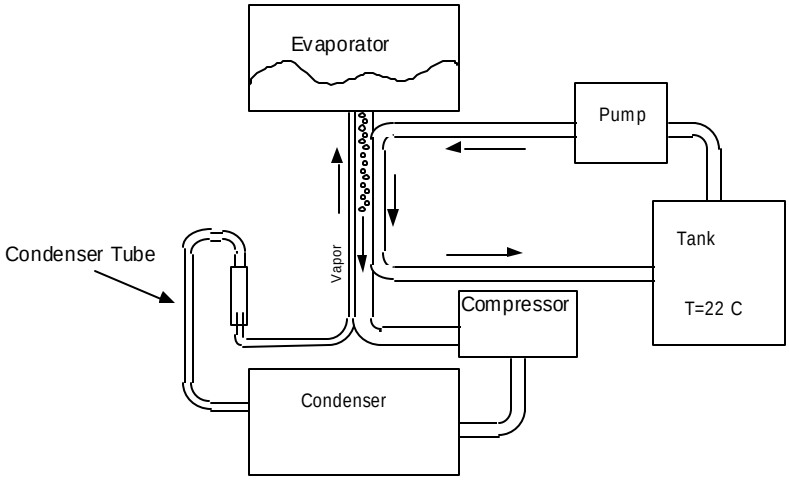

Figure 3.12

Figures 3.13a and 3.13b show the measured temperatures during the start cycle with and without the warming of the suction line heat exchanger. The figures shows approximately where a pop was heard. Comparing the graphs, notice that running heat transfer fluid through the warming tube did not have much affect on the inlet and outlet conditions of the capillary tube. In particular, notice in Figure 3.13a how the middle of the capillary tube (CT Mid - located on the surface of the capillary tube in the middle of the suction line heat exchanger) remains at a low temperature and even drops in temperature through the "popping" region. Looking at the middle of the capillary tube on Figure 3.13b, notice how the temperature begins to rise before the popping region. The warmed tube no longer presents the conditions needed to support condensation induced shock. To be sure that vibrations from running room temperature coolant through the tube did not upset the "popping", one test was run with -18° C coolant running through the connected pipe. The "popping" event occurred as normal for this case.

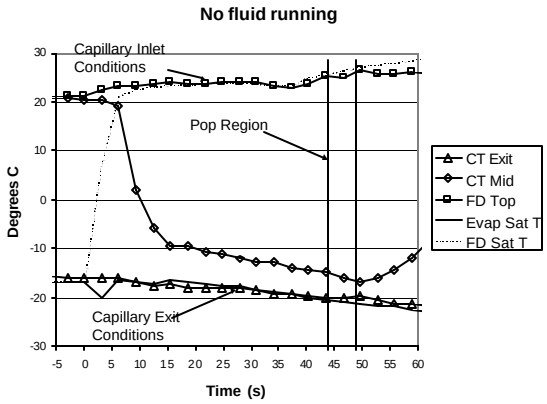

Figure 3.13a - No warming case

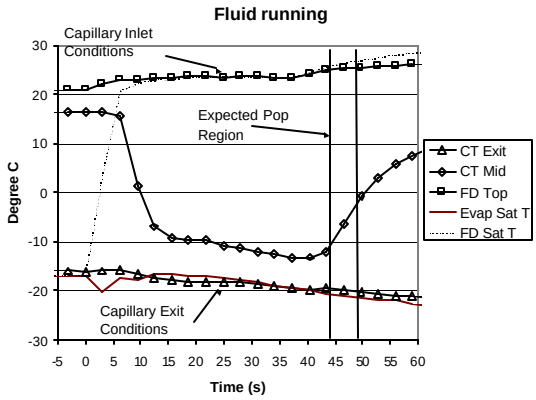

Figure 3.13b - Warming case

Chapter 4

4.0 Experimental Test Apparatus

4.1 Experimental Apparatus

In order to study the hypothesis presented in section 3.4 in a controlled way, the apparatus sketched in figure 4.1 was constructed. The apparatus uses a 30 lb tank of R134A refrigerant in a heated bath to provide a source of refrigerant at the desired temperature and pressure. The bath was well insulated and the liquid agitated to better control the refrigerant temperature and pressure. Both liquid and vapor valves on the refrigerant tank were used to feed refrigerant into a chamber meant to recreate the essential features for the filter dryer.

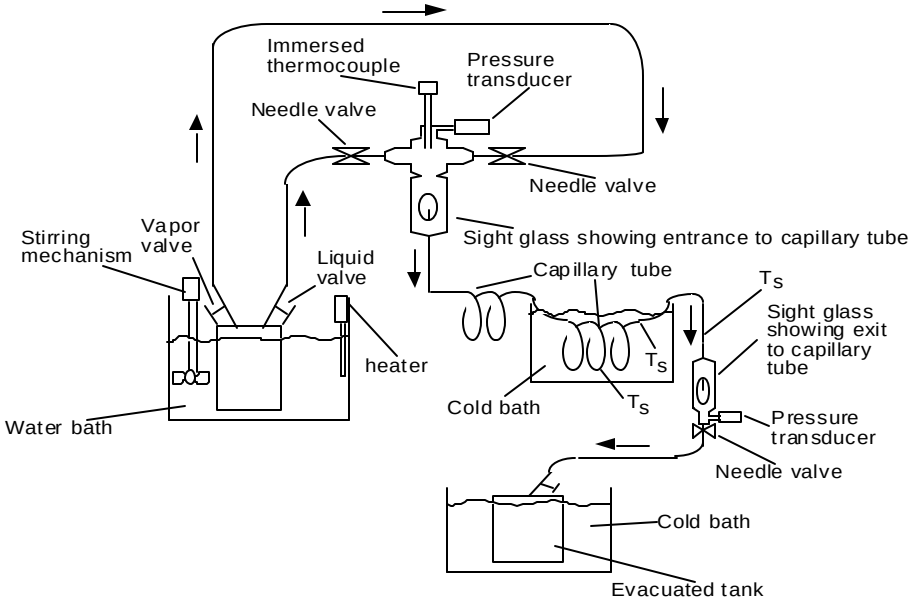

Fig. 4.1 - Apparatus for generating controlled “pops”

A picture of the simulated filter dryer is shown in figure 4.2. The center sight-glass allowed the capillary tube inlet to remain visible. Needle valves controlled the amount of vapor and liquid entering the filter dryer. An immersed thermocouple and pressure transducer record pressure and temperature at the inlet of the capillary tube. The simulated filter dryer could now control the essential features of the capillary inlet flow. The bath temperature of the refrigerant tank could be changed to control the inlet pressure. The needle valves could then control whether vapor or liquid entered the filter dryer.

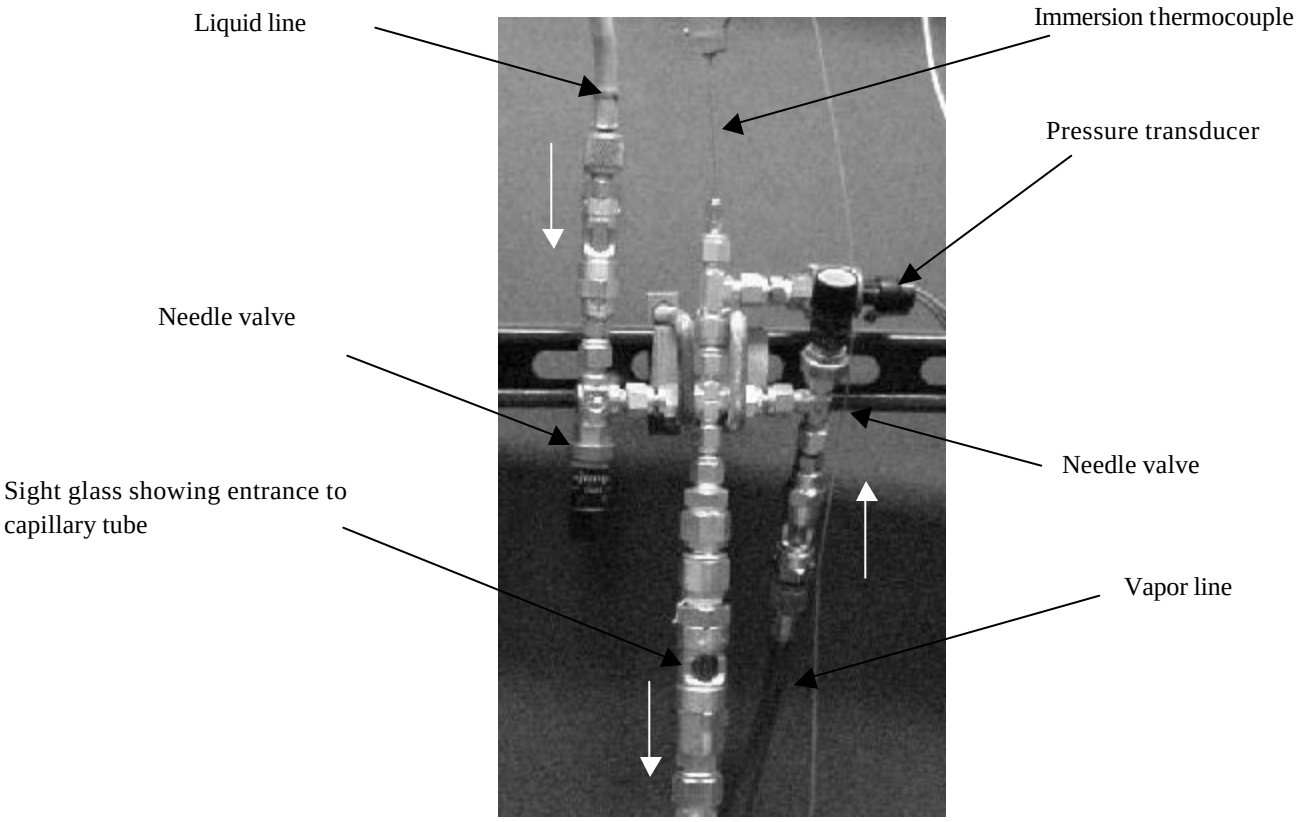

Fig. 4.2 - Simulated filter dryer

The capillary tube emerges from the bottom of this simulated filter dryer. The first 52 inches of the capillary tube is adiabatic. The next 59 inches of the tube was immersed in a chilled bath of coolant and the last nine inches were adiabatic and insulated. These lengths correspond to the length of each section for the capillary tube on the original refrigeration unit. The last nine inches were insulated because on the original refrigeration unit this length is in the freezer compartment and thus interacts with much colder air.

The cold bath simulated the effect of the drop in temperature of the suction line heat exchanger. The surface temperature of the capillary tube was dropped to temperatures corresponding to the data taken from the real refrigeration system. The bath was agitated to allow better control of the capillary surface temperature. Surface thermocouples were placed at various spots along the capillary tube. Table 4.1 list locations of all thermocouples.

Table 4.1

Overall Thermocouple position	Thermocouple type	Graphing name	Specific Location
Simulated filter dryer	Immersed, T type	CT in Imm	Center of flow 5 inches before capillary tube inlet at the junction between inlet vapor and liquid flows
Adiabatic capillary tube inlet	Surface, T type	CT Inlet	Surface of capillary tube, 9 inches downstream from the inlet
Simulated suction line heat exchanger	Surface, T type	CTE Imm	Surface of capillary tube, 5 inches upstream from end of heat exchanger section
Simulated suction line heat exchanger	Surface, T type	CT Mid Imm	Surface of capillary tube, the approximate center of heat exchanger section
Adiabatic outlet	Surface, T type	CT Ex	Surface of capillary tube, 6 inches upstream from capillary tube exit
Chilled tank	Immersed, T type		In chilled tank, approximately 5 inches from any part of the immersed capillary tube

The exit of the capillary is visible through a sight glass, which allowed knowledge of the refrigerant state. A pressure transducer followed the sight glass allowing the down stream pressure to be monitored. The downstream refrigerant then exhausts into a cold, evacuated refrigerant tank through a metering valve used to control the downstream pressure.

The shock wave was measured at the capillary tube exit by a differential pressure transducer. The pressure transducer was mounted flush with the inside wall of the exit sight glass. Figure 4.3 shows a diagram of how the transducer was mounted. This setup allowed the shock wave to be measured only when liquid filled the sight glass. Liquid coupling between the exit of the capillary tube and the pressure transducer was necessary for the pressure pulses to be measured. When vapor was present in the sight glass, the shock wave could be felt along the capillary tube, but the pressure transducer didn't measure it. Vapor dissipated the shock, thus stopping it from traveling further, but the capillary tube was still excited.

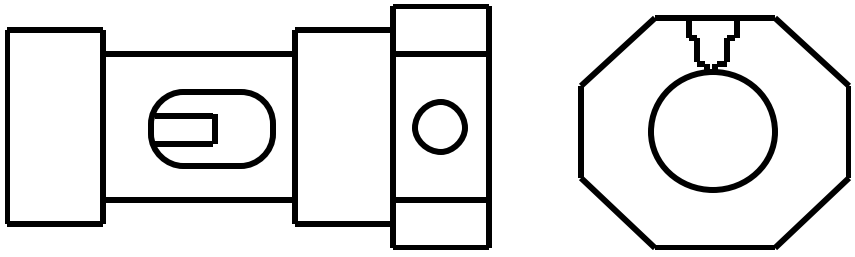

Figure 4.3 - Diagram of pressure transducer mounting

An accelerometer was attached to the surface of the capillary tube near the exit and was successful in measuring the shock waves whether vapor or liquid was present in the sight glass. An important distinction to make

here is that liquid refrigerant exited the capillary tube at all times whether the sight glass was filled with liquid or vapor. Liquid or vapor was then present in the sight glass depending on the pressure in the sight glass and how fast the liquid was allowed to drain away.

4.2 Experimental results

The sight glass at the inlet to the capillary tube allowed the state of the refrigerant entering the capillary tube to be witnessed. As witnessed in the clear filter dryer on the original refrigerator system, a vortex formed at the inlet when two phase refrigerant was present at the inlet. As the surface of the pooling refrigerant covered the inlet to the capillary tube, a vortex would form as long as the surface remained within a certain distance to the capillary tube inlet. The needle valves on the simulated filter dryer could be used to control the height of the liquid surface. Opening the vapor valve farther would allow more vapor to enter the filter dryer and the liquid surface would lower moving closer to the capillary tube inlet, while opening the liquid valve farther would have the opposite effect of raising the liquid surface away from the inlet. Figure 4.4 is a picture of the vortex as seen through the sight glass at the inlet to the capillary tube.

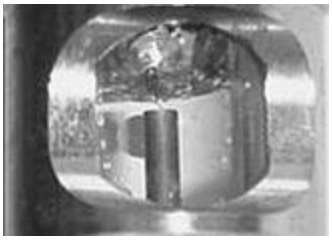

Figure 4.4 - Capillary tube inlet vortex

By changing the submergence of the capillary tube inlet, the vortex flow at the capillary tube inlet would change. Figure 4.5 is a visual depiction of how the surface vortex changed as the submergence of the capillary tube increased (the liquid surface rising farther away from the inlet). Picture A represents a large vortex that seemed to dip into the capillary tube. As the surface was raised to picture B, the vortex narrowed and appeared to spin faster. A long thin vapor core reached the entrance of the capillary tube. At picture C, a dimple depression would appear on the surface of the liquid. At random times a bubble would pull away from the dimple and enter the entrance to the capillary tube. At picture D, the submergence depth has increased to a point where no vortex phenomena was present and only liquid enters the capillary tube. In the no vortex case, it is unclear whether the liquid swirled while entering the capillary tube. These observations are identical to the observations of Takahashi et al. (1988), who described a similar application that is discussed in section 2.3.

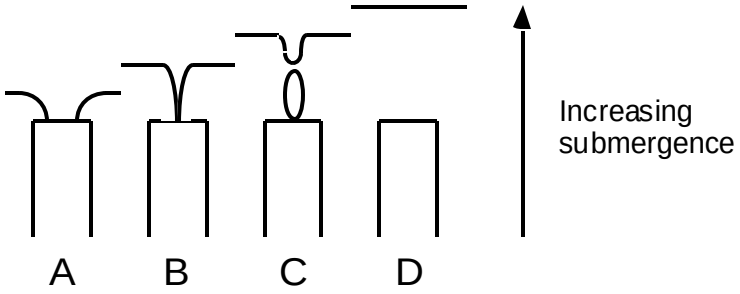

Figure 4.5 - Vortex dependence on submergence

Vortex phenomena type C was very important to the "popping" problem. Pressure pulses were regularly detected by the differential pressure transducer and the accelerometer during this type of vortex flow. To search for pressure pulses, the surface of the liquid would originally be brought to a position just above the inlet to the capillary tube. By adjusting the amount of liquid and vapor entering the simulated filter dryer, the surface of the liquid was made to steadily rise, which increased the submergence of the capillary tube inlet. The vortex phenomena would then move through the 4 flows previously described. As the flow transitioned to flow picture C, pressure pulses would begin being measured by the pressure transducer. A visual confirmation could be seen between a bubble being ingested, like picture C, and a pressure pulse being measured at the exit.

Shock waves were easily produced as long as the chilled bath was sufficiently cold. An attempt to quantify the relationship between bath temperature, capillary tube temperature, and inlet saturation temperature was made. The results were not reproducible with this apparatus. This apparatus supplied the important observation that the shock waves were only produced for specific vortex conditions at the inlet.

Figure 4.6 and 4.7 represent temperature profiles of the experimental apparatus. CT in Imm represents the saturation temperature at the inlet to the capillary tube or the saturation temperature in the simulated filter dryer. CTE Imm, CT Ex, CT Mid Imm, and CT Inlet are all surface thermocouples placed along the capillary tube. CTE Imm and CT Mid Imm are placed along a section of the capillary tube that is immersed in the cold bath or is part of the simulated suction line heat exchanger. The plot shows that all temperatures are in a steady state condition. "Shocks" were not detected through out this period. They were only detected in the marked region.

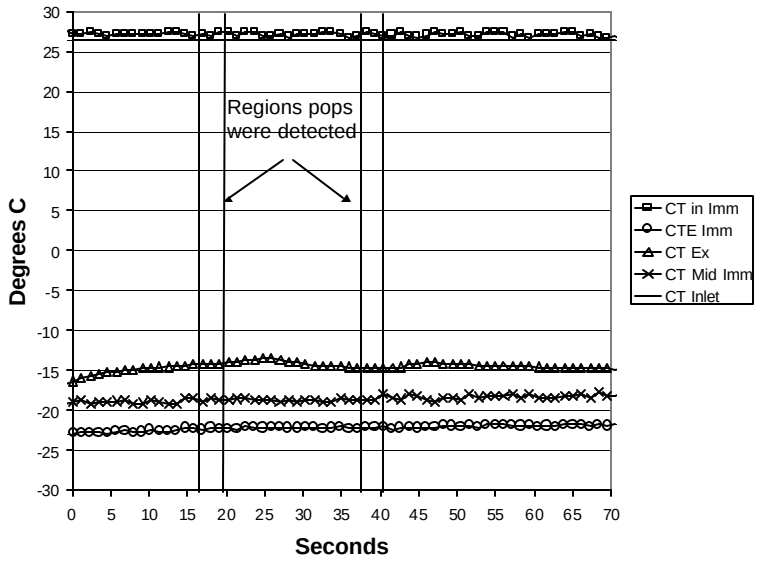

Figure 4.6 - Temperature profile of apparatus with “popping” regions

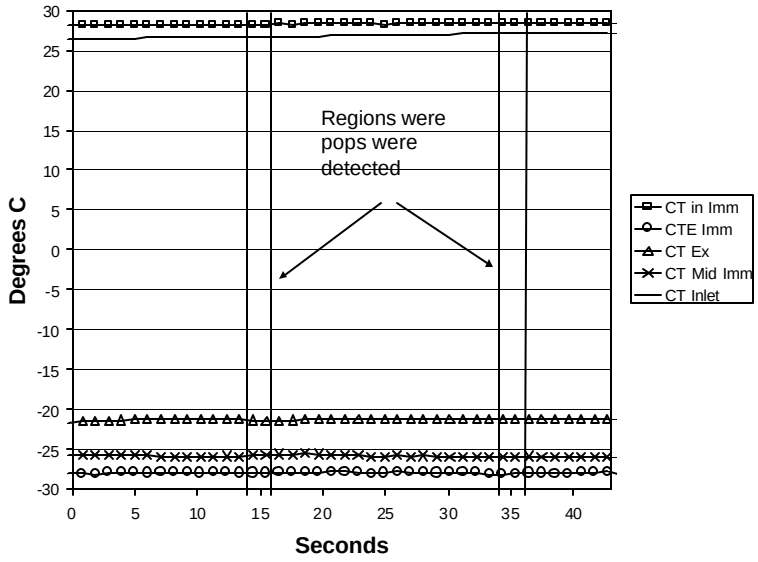

Figure 4.7 - Temperature profile of apparatus with “popping” regions

It appears that having the necessary pressure and temperature conditions for the shock to occur is not enough. The temperatures were controlled to conditions that would represent the temperatures and pressures seen by the capillary tube on the actual refrigerator. The valves that control the amount of vapor and liquid entering the simulated filter dryer were then used to form a vortex. The vortex was then manipulated to the regime that allowed ingestion of vapor bubbles. After the vortex was moved to its proper regime, shock waves would be detected by the down stream differential pressure transducer or the accelerometer. If a vapor bubble is not ingested at the inlet, condensation induced shock does not occur and thus a shock wave is not present.

The bubble entrainment regime did not seem to be a stable equilibrium. Usually upon reaching the bubble entrainment regime, after about 5 to 10 seconds, the vortex would either migrate to the all liquid regime or to the steady vapor core regime. On figure 4.6 and 4.7 this represented the time elapsed in the popping region. After that time, the vortex had moved away from the proper regime and did not begin entraining bubbles until the second popping region.

Chapter 5

5.0 Experimental Test Apparatus

Studying the relationship between upstream pressure and tank temperature for the previous experimental set-up led to results that were not reproducible. A change was made to the set-up in an attempt to run a more reproducible experiment. This second apparatus allowed us to explore important temperatures and pressures associated with "popping".

5.1 Apparatus II

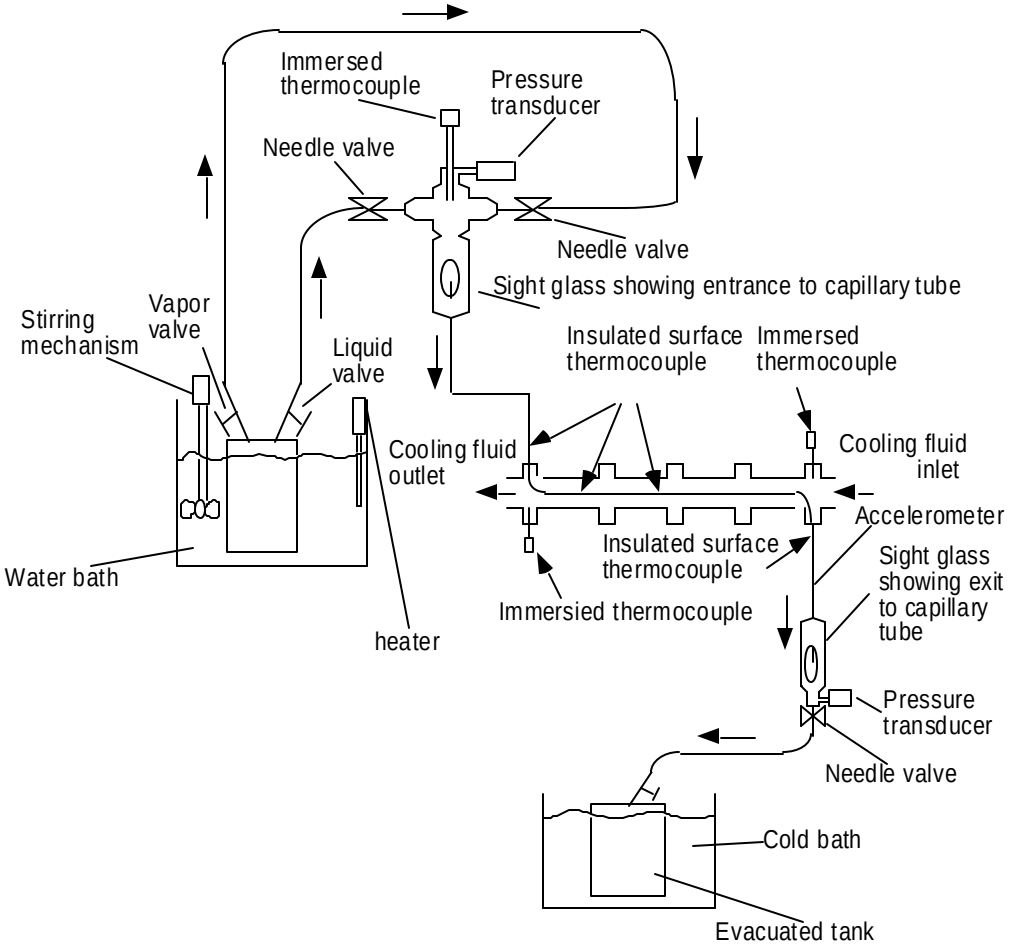

Figure 5.1 - Experimental set-up with counter flow heat exchanger

Figure 5.1 depicts the new experimental setup. The new setup uses the same refrigerant source and simulated filter dryer as the previous setup. The inlet conditions, including the inlet vortex, could be controlled the same way as in the previous experiments. This setup uses a counter flow heat exchanger to simulate the suction line heat exchanger. Well-insulated thermocouples were placed along the length of the capillary tube to try to determine the internal temperature of the fluid. Immersed thermocouples were also placed in the cooling fluid flow to

determine if any appreciable temperature drop can be detected. This setup relies on an accelerometer to detect passing shock waves.

Figure 5.2 shows a more detailed depiction of thermocouple positions. The thermocouple positions are numbered and table 5.1 gives specific information about each position. Position 1 measures the internal simulated filter dryer temperature. Well-insulated surface thermocouples follow the rest of the length of the capillary tube and give an approximation of the internal fluid temperature. With an inside diameter of 0.036" and outside diameter of 0.089", conduction through the capillary tube wall may not be negligible. The conduction is not taken into account in the approximate internal fluid temperatures and that fact should be remembered when reviewing the data.

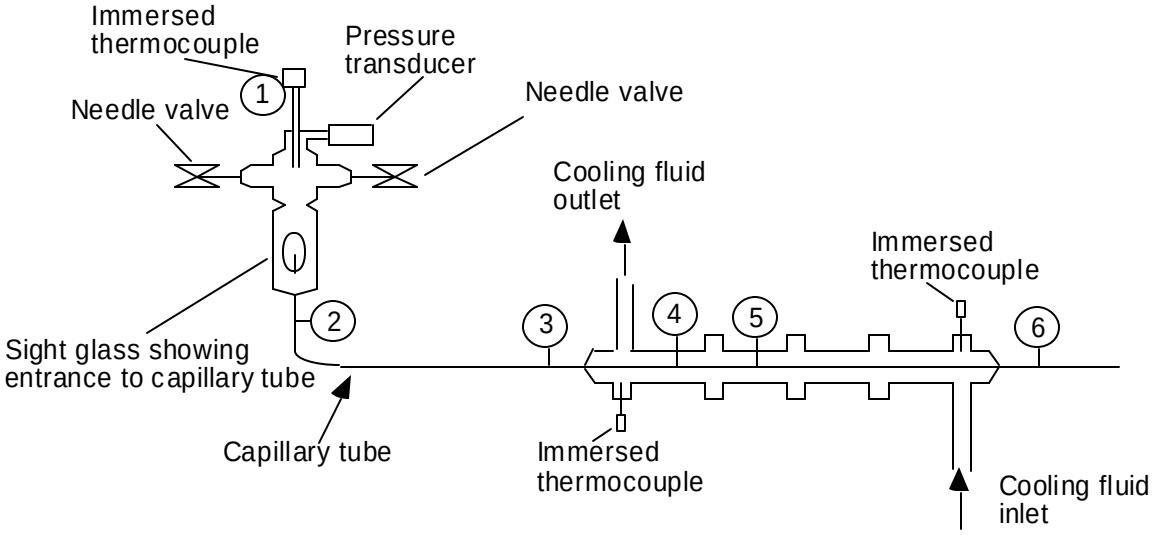

Figure 5.2 - Detailed view of thermocouple positions

Table 5.1

Thermocouple position	Type	Specific location
Position 1	Immersed, T-type	Entrance to simulated filter dryer
Position 2	Surface, T-type	10" from inlet to capillary tube
Position 3	Surface, T-type	47" from inlet of capillary tube, 3" before heat exchanger
Position 4	Surface, T-type	59" from inlet of capillary tube, 9" from start of heat exchanger
Position 5	Surface, T-type	73" from inlet of capillary tube, 23" from start of heat exchanger
Position 6	Surface, T-type	110" from inlet of capillary tube, 10" form exit of capillary tube
Cooling fluid outlet	Immersed, T-type	Start of heat exchanger section
Cooling fluid inlet	Immersed, T-type	End of heat exchanger section

5.2 Experimental Results

Experiments were conducted to determine the relationship between temperature of the cooling fluid in the simulated suction line heat exchanger and the presence of the "popping" event. Upstream pressures of 80, 100, and 120 psi were maintained while varying the cooling fluid temperature to determine how warm the cooling fluid could be before the "popping" ceased to occur.

The tests began with the cooling fluid at -20° C where the "popping" event is easily detected at all three inlet pressures. The cooling fluid was then allowed to slowly warm up. For approximately every 1 or 2° C that the cooling fluid warmed up, a check for the presence of the "popping" event was made. As in the last apparatus, the inlet vortex conditions were very important to the "popping" event. If the proper vortex regime was not present at the inlet to the capillary tube, then no "popping" occurred. An accelerometer placed at the exit of the capillary tube was used to detect "popping". By this method, a relationship between inlet pressure, cooling fluid temperature and the presence of pops could be explored.

Figures 5.3 to 5.5 give the results of the testing. The independent axis is represented by fluid inlet temperature and corresponds to the value of the cooling fluid entering the heat exchanger. The figures depict the temperature values of each thermocouple position for a given upstream pressure and cooling fluid entrance temperature. Three regions of relative pop strength are labeled on each figure. A general decline in pop strength occurred as the cooling fluid temperature increased. The labeled regions are relative and could have been placed differently. In the "no popping detected" region, infrequently very small impulses were detected but they were barely distinguishable from the flow noise at the exit and therefore for all practical purposes the "popping" had ceased. The cooling fluid outlet temperature is not shown on the graphs because the temperature difference between the cooling fluid entrance and outlet was less then 0.5° C and is therefore influenced by the accuracy of the instrumentation.

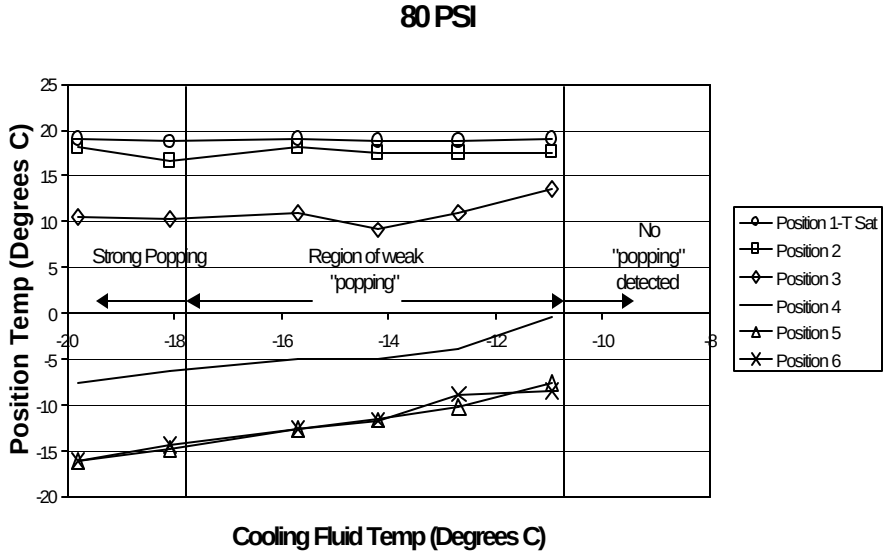

Figure 5.3 - Position temperatures for inlet pressure of 80 psi

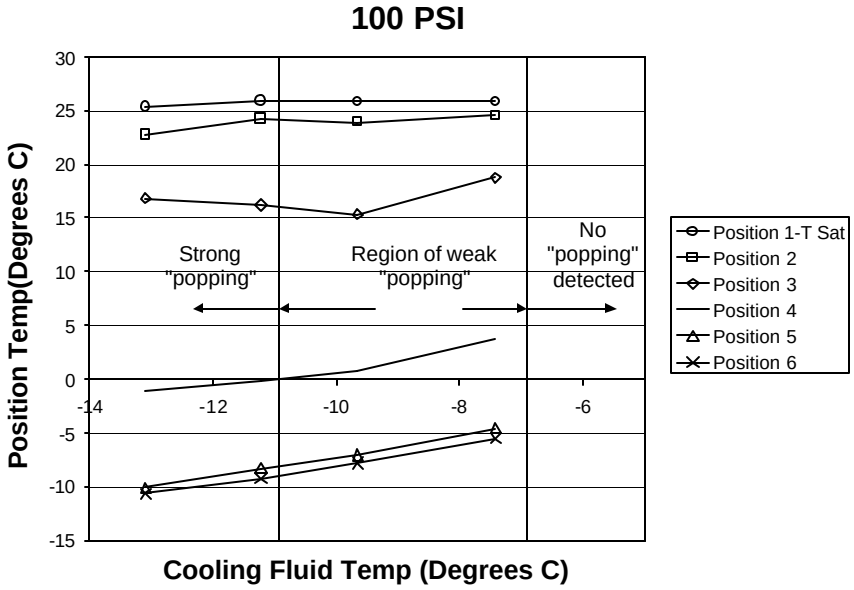

Figure 5.4 - Position temperatures for inlet pressure of 100 psi

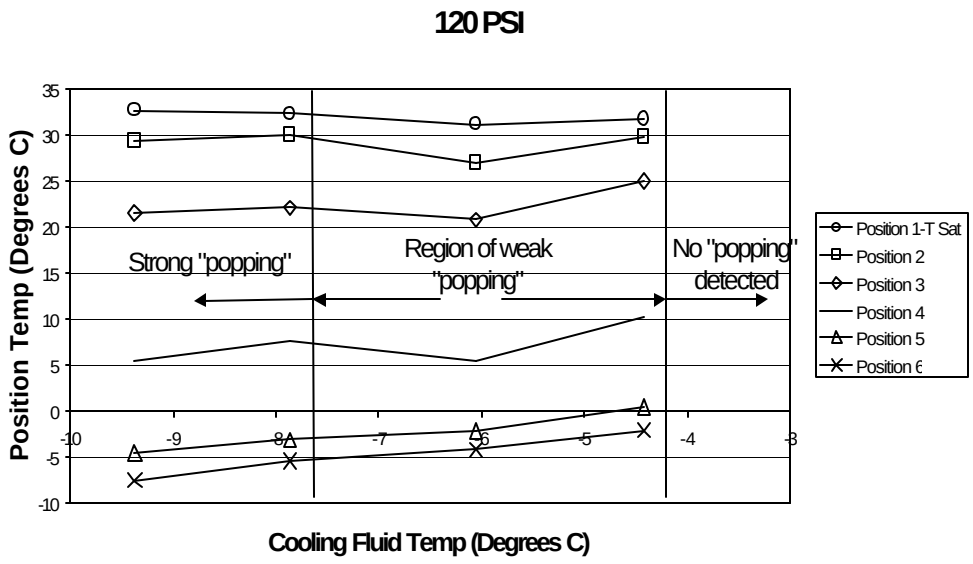

Figure 5.5 - Position temperatures for inlet pressure of 120 psi

Comparing figure 5.3 through 5.5, some simple observations can be made. The temperature at position 3 gives the approximate temperature inside the capillary tube just before it enters the heat exchanger and position 6 gives the approximate temperature inside the capillary tube as it exits the heat exchanger. Position 6 is thus approximately the final temperature at the exit of the capillary tube.

Comparing position 4 and 5 to position 3 and 6 shows that the approximate temperature inside the capillary tube drops quickly upon entering the heat exchanger. The temperature drop between position 5 and 6 is on average less then one degree but the distance between them represents about 54% of the capillary tube length in the heat

exchanger. For example, looking at the third data point on figure 5.4, the capillary length between position 3 and 4 represents 21% of the heat exchanger length and 62% of the temperature drop. Similarly, the capillary length between position 4 and 5 represents 24% of the heat exchanger length and 33% of the temperature drop. Thus, most of the heat transfer occurs rapidly in the first half of the heat exchanger.

Another trend visible from figures 5.3 to 5.5 is that as the upstream pressure increases the chilling fluid temperature that supports "popping" increases. The no popping region for 80, 100, and 120 psi began at -11, -7, and -5 respectively. A possible explanation for this trend is that condensation induced shock is the "popping" mechanism. As discussed in section 4.2, a bubble is entrained in this apparatus by controlling the vortex at the inlet. We will assume that while the bubble travels through the adiabatic section of the capillary tube that the vapor in the bubble remains at saturated conditions while the pressure drops. It is possible that as the bubble moves down the adiabatic section of the capillary tube it grows in size due to flashing of the refrigerant. As the bubble enters the heat exchanger, good heat transfer between the tube walls and the surrounding liquid refrigerant drops the temperature around the bubble quickly. The temperature difference between the vapor and the surrounding liquid would be a factor in the potential of the bubble to suddenly collapse as in condensation induced shock. The difference in temperature of the vapor bubble and the surrounding liquid may cause the upstream pressure and chilling fluid temperature relationship shown in Figures 5.3 to 5.5.

5.3 Calculations

By assuming that incompressible liquid refrigerant is flowing the entire length of the capillary tube, a simplified look at the flow through the capillary tube from a theoretical basis can be made. The forces acting on a fluid through a completely filled horizontal pipe are inertia, viscous, pressure, and elastic (Marks Handbook, 1996). For Reynolds numbers greater then 4000, the flow is considered turbulent. Later we will show that the Reynolds number for the capillary tube falls in the turbulent regime. In the absence of disturbances, the flow could be in a metastable laminar flow condition. The exact flow conditions are unknown and will be considered turbulent for these calculations. For turbulent flow in a pipe the friction factor varies according to the Colebrook equation:

$$\frac{1}{\sqrt{f}} = -2\log_{10}\left(\frac{e/d}{3.7} + \frac{2.5}{R\sqrt{f}}\right) \qquad (1)$$

where: f = friction factor
ε = surface roughness
d = pipe diameter
R = Reynolds number

From experiments, the pipe geometry and total pressure drop are known and allow the head loss and friction factor to be established.

Neglecting head losses due to gravity, the head loss can be calculated using:

$$h = \frac{(p_1 - p_2)}{rg} \qquad (2)$$

where: h = head loss
p_1,p_2 = pressure
ρ = density
g = gravity

Now the Colebrook equation can be solved to determine the friction factor by substituting:

$$e/d \tag{3}$$

where: ε = surface roughness of capillary tube = $1.524\times10^{-6}\,m$ (Mark's Handbook, pp. 3-48)

and $$R\sqrt{f} = \frac{rd}{m}\left(\frac{2ghd}{2}\right)^{1/2} \tag{4}$$

The friction factor allows the average velocity and mass flow to be found by:

$$V = \left(\frac{2gh}{K_{in} + K_{out} + \frac{fL}{d}}\right)^{1/2} \tag{5}$$

where: V = refrigerant velocity
K_{in} = resistance coefficient of capillary tube inlet = 1 (Mark's Handbook, pp. 3-51)
K_{out} = resistance coefficient of capillary tube outlet = 1 (Mark's Handbook, pp. 3-51)
L = length of pipe

$$\dot{m} = rVA \tag{6}$$

where: $\dot{m}$ = mass flow rate

The above equations can then be solved for the inlet conditions 80, 100, and 120 psi. An average of the density and viscosity at the known inlet and exit conditions were used for calculations. The calculation results are summarized in table 5.2. Notice that the Reynolds numbers are greater than 4000 so the assumption of turbulent flow is reasonable. However, laminar flow can be achieved at much higher Reynolds number than 4000 in the absence of disturbances. Metastable regions in capillary tube flow do exist and have been the topic of much study.

The assumption of liquid flow down the capillary tube may not be true. In the actual capillary tube, the refrigerant may flash before reaching the suction line heat exchanger or it may stay in a metastable liquid state even though the pressure falls below the saturation pressure of the liquid refrigerant. Even if the refrigerant flashes, it will recondense quickly after entering the heat exchanger. This might be a mechanism for condensation induced shock. Also, near the exit of the capillary tube the pressure drops low enough that a small portion of the refrigerant may flash. These limitations are not negligible, but the above simplification is still meaningful. Experimental measurements of mass flow for 100 and 120 psi can be found in appendix A. Values of 1.63 g/s and 2.0 g/s were found for 100 and 120 psi respectively. Flashing refrigerant choking the flow and also experimental limitations may have caused the reduced values found experimentally.

Table 5.2

Inlet Pressure (Psi)	Head Loss (m)	Reynolds #	Velocity (m/s)	$\dot{m}$ (g/s)	friction factor
80	35.2	8175	2.418	2.07	0.03484
100	46.46	9780	2.832	2.39	0.03349
120	57.92	11255	3.209	2.69	0.03252

The calculations can be used to get an estimate of the pressure along the entire length of the capillary tube. The calculated pressures can then be used to investigate the experimental data further. If a vapor bubble was ingested at the capillary tube entrance and traveled into the suction line heat exchanger for some distance without condensing, the liquid temperature surrounding the bubble may drop much faster then the bubble temperature. The bubble would then find itself surrounded by increasingly sub-cooled liquid. Recalling from the experimental data, the temperature at position 5 has dropped to almost the temperature measured at the exit of the heat exchanger. Therefore position 5 gives an estimate of the maximum possible sub-cooling of the surrounding liquid. The liquid temperature could not drop much colder then the position 5 temperature.

The above described situation would lead to a vapor bubble at the saturation conditions found at position 5 surrounded by sub-cooled liquid. Using the experimental temperature measured at position 5 and the calculated position 5 pressure, the Jakobs number can be calculated using:

$$Ja = \frac{r_L c_L (T_S - T_L)}{r_G h_{fg}}$$

where: ρ_L = density of liquid
ρ_G = density of gas
h_{fg} = latent heat
c_L = specific heat of liquid
T_s = saturation temperature
T_L = temperature of liquid

Recall from section 2.1.1 that the Jakobs number relates the rate that heat can leave the bubble to the rate of heat that needs to be rejected to condense the vapor. A Jakobs number greater then 1 indicates that heat can be drawn away faster than what is needed to condense the vapor. To calculate the Jakobs number, the density of the gas is the saturated vapor density of the refrigerant at the saturation pressure calculated. Also, the density and specific heat of the liquid is found at the calculated pressure and measured temperature.

Figure 5.6 represents a plot of Jakobs number vs. cooling fluid inlet temperature for inlet pressures of 80, 100, and 120 psi. The plot shows the Jakobs number for inlet pressures of 80, 100, and 120 psi as the cooling fluid inlet temperature warms up. As the cooling fluid inlet temperature warms, the Jakobs number decreases until "popping" no longer exists. The plot is divided into a "popping" and "no popping" region. In the "popping" region the relative strength of "popping" decreased with decreasing Jakobs number. The results show that for this apparatus that as the Jakobs number reaches approximately 8, the system can no longer support "popping".

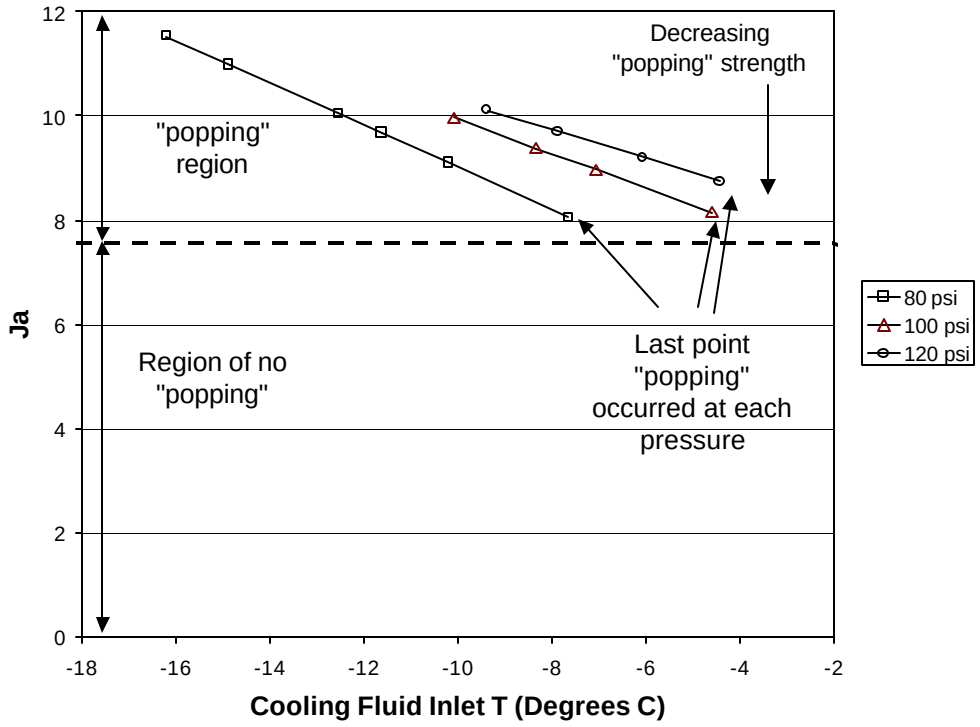

Figure 5.6 - Ja vs. Cooling Fluid Inlet T

The above plot suggests that with simple instrumentation the ability of the system to support “popping” can be determined. For the apparatus by measuring the high and low side pressure and the surface temperature of the capillary tube approximately in the middle of the suction line heat exchanger, we can predict the likelihood of “popping” to occur. In section 3.6.2, the suction line heat exchanger was warmed at the start of the compressor on cycle to suppress the event. We can go back and look at the data and determine the Jakobs number for each case. Figures 5.7a and 5.7b show the plot of the data for warming and no warming. Recall that the capillary inlet and outlet conditions were not changed significantly by the warming. The difference in the two plots is how cold the capillary tube middle temperature is during the “popping” and expected “popping” region.

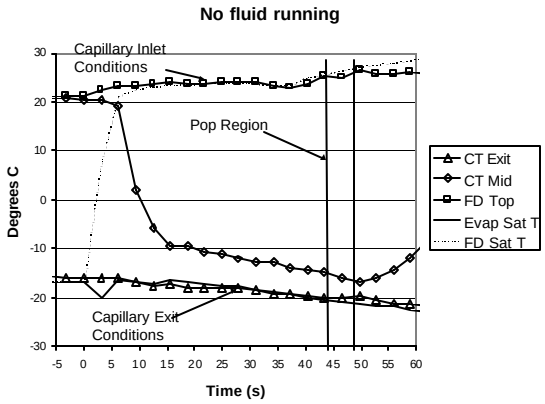

Figure 5.7a - Normal cycle

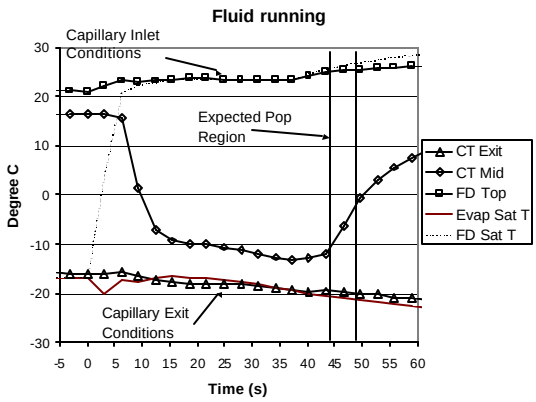

Figure 5.7b - Warmed cycle, no "popping"

CT Mid is a surface thermocouple on the capillary tube half way along the suction line heat exchanger. Using the CT Mid temperature found at the center of the "popping" region and expected "popping" region along with the calculated pressure from the Colebrook equation at that position, the Jakobs number can be determined. The result was a Jakobs number of 11.9 for the normal cycle and 8.5 for the warmed cycle. Looking back at figure 5.6 a value of 11.9 is well into the "popping" region and we would expect that if the right capillary tube inlet vortex condition existed "popping" would occur. The value of 8.5 is near the edge of the no "popping" region and we would expect very light "popping" if any at all.

The experimental apparatus was designed to simulate the refrigerator previously used for experiments. Other refrigerators may have a different relationship to specific Jakobs number due to differences in the refrigerator components. Experimental work would need to be done to determine that relationship.

Chapter 6

6.0 Conclusion

The "popping" noise reported to occur in household refrigerators was experimentally investigated. The results led to the hypothesis of condensation induced shock as the root cause. This hypothesis was supported by experimental results involving a "popping" refrigerator and experimental apparatuses designed to simulate the important aspects of the pop.

A refrigerator that experienced the "popping" noise was instrumented to determine the operating conditions leading to the event. The "pop" was found to occur at the beginning of the compressor on cycle when refrigerant migration causes large temperature and pressure transients. The drop in temperature of the suction line heat exchanger and vortex formation at the inlet were identified as key phenomena for the "popping" to occur. Further experiments verified the importance of the vortex at the capillary tube inlet and drop in temperature of the suction line heat exchanger to the "popping" event. Condensation induced shock, caused by bubbles being entrained by the vortex at the capillary tube inlet reaching the very cold suction line heat exchanger and collapsing, was identified as a possible cause. Condensation induced shock (CIS) occurs when a vapor bubble is suddenly surrounded by sub-cooled liquid causing the bubble to collapse quickly resulting in a shockwave. Heat transfer and inertia determine the strength of the shock.

An experimental apparatus was made to simulate the conditions in and around the refrigerator's capillary tube during the "popping" event. Controlling the amount of vapor and liquid entering a simulated filter dryer allowed some control of the vortex at the inlet of the capillary tube, which was visible through a sight glass. "Popping" would only occur under specific inlet vortex conditions even while the rest of the capillary tube conditions were held constant. The pressure pulse was found to travel through liquid refrigerant inside the capillary tube and through the metal of the tube. The pressure pulse was measured by a surface accelerometer and a differential pressure transducer in the flow at the exit of the capillary tube. Liquid refrigerant at the exit was necessary to couple the pulse to the pressure transducer. When liquid was not present the pulse was dissipated and not detected by the differential pressure transducer. The surface accelerometer would detect the pulses even without a liquid seal at the exit.

A second apparatus was built to explore the relationship between suction line heat exchanger temperature and the event. The heat exchanger temperature began at -20° C and was slowly warmed until the "popping" event ceased to occur. The capillary tube temperature dropped very quickly upon entering the heat exchanger. 62% of the temperature drop occurred in the first 21% of the suction line heat exchanger capillary tube length. The experiments showed that as upstream pressure increases the chilling fluid temperature that supports "popping" increases.

Assuming incompressible liquid refrigerant down the length of the capillary tube, the pressure along the capillary tube was calculated using the Colebrook equation. This allowed the calculation of the Jacobs number between a vapor bubble at the calculated saturation pressure and sub-cooled liquid at the measured capillary tube temperature. A relationship between Jacobs number and presence of "popping" was obtained. This relationship was applied to the refrigerator experiments and good agreement was found.

The “popping” problem is strongly related to the suction line heat exchanger temperature drop and the capillary tube inlet vortex condition. More work needs to be done to determine how to eliminate the capillary tube inlet vortices to prevent bubble entrainment. Also, the Jakobs number has been shown to be a possible measure of the likelihood of “popping” occurrence. Simple instrumentation can be used to establish the Jakobs number. More work needs to be done to generalize the relationship between the Jakobs number and “popping”.

The two important events found to contribute to the “popping” problem are summarized below:

- Bubbles reaching the suction line heat exchanger

  Bubbles are entrained in the refrigerant flow by a vortex at the entrance to the capillary tube. Stopping formation of the vortex may be enough to stop “popping”. A second possible mechanism could be flashing of refrigerant in the adiabatic section of the capillary tube, but this was never observed in experiments.

- Bubble being surrounded by sub-cooled liquid

  The bubble needs to become surrounded by sub-cooled liquid for condensation induced shock to occur. The drop in temperature of the suction line heat exchanger may cause the liquid surrounding the bubble to become sub-cooled. The necessary amount of sub-cooling can be estimated by the Jakobs number, which can then be used to indicate “popping” conditions.

References

Belytschko, T., Karabin, M., and Lin, J. I., 1986. "Fluid-structure interaction in waterhammer response of flexible piping." *Journal of pressure vessel technology*, Vol. 108, pp. 249-255.

Coulter, W. H. and Bullard, C. W., 1997. "An experimental analysis of cycling losses in domestic refrigerator-freezers." *ASHRAE Transactions*, Vol. 103[1], pp. 587-596.

Denny, D. F., 1956. "An experimental study of air-entraining vortices in pump sumps." Proceedings of the institution of mechanical engineers, Vol. 170[2], pp. 106-125.

Durgin, W. W. and Hecker, G. E., 1978. "The modeling of vortices at intake structures." Proceedings of the joint symposium on design and operation of fluid machinery, Vol. 1, pp. 381-391.

Florschuetz, L. W. and Chao, B. T., 1965. "On the mechanics of vapor bubble collapse." *Journal of heat transfer*, Vol. 87[2], pp. 202-220.

Gillessen, R. and Lange, H., 1988. "Water hammer production and design measures in piping systems." *International journal of pressure vessel and piping*, Vol. 33, pp. 219-234.

Hatfield, F. J., Wiggert, D.C., and Otwell, R. S., 1982. "Fluid structure interaction in piping by component synthesis." *Transactions of the ASME: Journal of fluids engineering*, Vol. 104, pp. 318-325.

Hatfield, F. J., and Wiggert, D. C., 1991. "Water hammer response of flexible piping by component synthesis." *Journal of pressure vessel technology*, Vol. 113, pp. 115-119.

Hunter, C., 1960. "On the collapse of an empty cavity in water." *Journal of fluid mechanics*, Vol. 8, pp. 241-262.

Hydraulic Institute Standards, 1983. "Centrifugal, rotary, and reciprocating pumps." 14th edition, Cleveland, Ohio, pp. 125-133.

Jacobi, A. M. and Shelton, J., 1995. "A fundamental study of refrigerant line transients." Master Thesis, University of Illinois, Champaign-Urbana, IL.

Jacobi, A. M., and Shelton, J., 1997. "A fundamental study of refrigerant-line transients: part 1 - description of the problem and survey of relevant literature." *ASHRAE Transactions*, Vol. 103 [1], pp. 1-12.

Kim, J. H., 1987. "Two-phase water hammer in nuclear power plants." *Cavitation and multiphase flow forum*, pp. 117-120.

Knauss, J., 1987 Swirling Flow Problems at Intakes: Hydraulic Structures Design Manual. A.A. Balkema, Rotterdam, Netherlands. pp. 1-11.

Marks' Standard Handbook For Mechanical Engineers, 10th edition, 1996. McGraw-Hill, New York, New York, pp. 3-47 to 3-51.

Rayleigh, Lord, 1917. "On the pressure developed in a liquid during the collapse of a spherical cavity." *Philosophical Magazine*, Vol. 34, pp. 94-98.

Rubas, P. J. and Bullard, C. W., 1995. "Factors contributing to refrigerator cycling losses." *International Journal of Refrigeration*, Vol. 18[3], pp. 168-176.

Sibetheros, I. A., Holley, E. R., and Branski, J. M., 1991. "Spline interpolations for water hammer analysis." *Journal of hydraulic engineering*, Vol. 117[10], pp. 1332-1351.

Singh, R., Nieter, J. J., and Prater, G., 1986. "An investigation of the compressor slugging phenomenon." *ASHRAE Transactions*, Vol. 92[1B], pp. 250-258.

Suo, L., Wylie, E. B., 1989. "Impulse response method for frequency-dependent pipeline transients." *Transactions of the ASME: Journal of fluids engineering*, Vol. 111, pp. 478-483.

Takahashi, M., InOue, A., and Aritomi, M., 1988. "Gas entrainment at free surface of liquid," *Jounal of Nuclear Science*, Vol. 25 [2], pp. 131-142.

Tsou, J. L., Melville, B. W., Ettema, R., and Nakato, T., 1994. "Review of flow problems at water intake pump sumps." *Heat exchanger technologies for the global environment: presented at 1994 international joint power generation conference. ASME power*, Vol. 25, pp. 91-102.

Walker, J. S. and Phillips, J. W., 1977. "Pulse propagation in fluid-filled tubes." *Journal of Applied Mechanics*, Vol. 44[1], pp. 31-35.

Wang, J. and Wu, Y., 1990 "Start-up and shut-down operation in a reciprocating compressor refrigeration system with capillary tubes." *International Journal of Refrigeration*, Vol. 13[3], pp. 187-190.

Wittke, D. D. and Chao, B. T., 1967. "Collapse of vapor bubbles with translatory motion." *Journal of heat transfer*, Vol. 89[1], pp. 17-24.

Wylie, E. B. and Streeter, V. L., 1978. Fluid transients. Mcgraw-Hill inc., USA, pp. 31-63.

Zwick, S. A. and Plesset, M. S., 1955. "On the dynamics of small vapor bubbles in liquids." *Journal of Mathematics and Physics*, Vol. 33, pp. 308-329.

Appendix A

Mass Flow

The mass flow of the apparatus discussed in section 5.1 was measured for upstream pressures of 100 and 120 psi. The mass flow was measured by maintaining constant conditions along the length of the capillary tube while the refrigerant was captured at the exit by a sampling tank. This method took advantage of the fact that most of the refrigerant leaving the capillary tube was liquid and therefore a large majority of the mass flow was liquid. Figure A-1 depicts the refrigerant sampling tank used to capture the refrigerant. The tank was immersed in glycol-water mixture that was held at -45° C to prevent the refrigerant from evaporating.

Mass flow for different cooling fluid temperatures at each upstream pressure were measured. The refrigerant was captured for a period of 12 minutes after which the sampling tank was closed off and weighed. The added mass was then averaged over the 12 minute period to determine the mass flow.

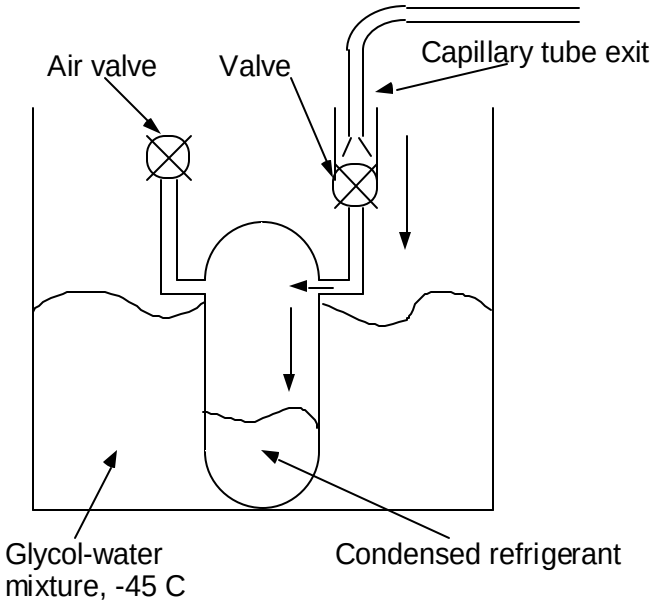

Figure A-1

Table A-1 gives the results for mass flow under different conditions. Cooling fluid temperatures of -20, -15, and -10 were tested. It is believed that cooling fluid temperature does not play a large role in mass flow over this range. However, the results were inconclusive. At sufficiently low cooling fluid temperatures it's believed that flashing of the refrigerant does not occur until the capillary tube exit. Lower cooling fluid temperature may allow for flashing to occur before the exit of the capillary tube, thus reducing the mass flow.

This flashing of refrigerant either at the exit or before the exit accounts for an error in the measurement. An unknown amount of refrigerant flashes at the exit and thus is not accounted for. The flashing refrigerant is believed to be a small part of the whole. The flashing refrigerant may play a large effect on mass flow if it caused choking, but that would not result in an error in these measurements. Also, sub-cooling at the inlet (listed in table A-1) was uncontrollable with this apparatus and affected the mass flow by an undeterminable amount.

Table A-1

Capillary tube inlet pressure (psi)	Cooling fluid inlet temperature (C)	Inlet sub-cooling (C)	Capillary tube exit surface temperature (C)	Mass Flow (g/s)
100 psi				
98.2	-20.1	1.44	-15.5	1.61
99.1	-14.8	0.05	-11.2	1.64
98.6	-9.8	0.53	-6.8	1.64
120 psi				
124.5	-20.2	0.87	-14.5	2.08
126.1	-15.4	2.84	-10.4	1.99
122.8	-10.5	1.88	-7.0	1.96